Auditory processing remains sensitive to environmental experience during adolescence

Kelsey L. Anbuhl[1], Justin D. Yao[1], Robert A. Hotz[1], Todd M. Mowery[1,5], Dan H. Sanes[1,2,3,4]

[1] Center for Neural Science, New York University, 4 Washington Place, New York, NY 10003
[2] Department of Psychology, New York University
[3] Department of Biology, New York University
[4] Neuroscience Institute at NYU Langone School of Medicine
[5] Department of Otolaryngology, Rutgers University

Contact: Kelsey L. Anbuhl: kla7@nyu.edu; Dan H. Sanes: dhs1@nyu.edu

Pages 43
Figures 11 (8 main figures, 3 supplemental)
Tables 0

Key Words
hearing loss, auditory cortex, auditory perception, developmental plasticity

Abbreviations
auditory cortex (AC), hearing loss (HL), amplitude modulation (AM), inhibitory postsynaptic potential (IPSP), excitatory postsynaptic potential (EPSP)

Acknowledgements
This work was supported by NIMH T32-MH019524 (KLA), NIDCD F32-DC018195-02 (KLA), and NIDCD R01-DC011284 (DHS). We would also like to acknowledge the Endocrine Technologies Core (ETSC) at the Oregon National Primate Research Center (ONPRC), which is supported by NIH Grant P51 OD011092 (ONPRC). We thank Lisa Ramirez for assistance in histological preparation and analyses. We are grateful to Melissa Caras and members of the Sanes lab for support and insightful feedback regarding analysis and interpretation of data.

Author Contributions
KLA and DHS designed research and secured funding; KLA collected behavioral and *in vivo* physiological data; RAH collect behavioral control data; TMM collected *in vitro* physiology data; KLA, TMM, and JDY analyzed data. KLA and DHS wrote manuscript.

Conflict of interest
The authors declare no competing financial interests.

Abstract

Development is a time of great opportunity. A heightened period of neural plasticity contributes to dramatic improvements in perceptual, motor, and cognitive skills. However, developmental plasticity poses a risk: greater malleability of neural circuits exposes them to environmental factors that may impede behavioral maturation. While these risks are well-established prior to sexual maturity (i.e., critical periods), the degree of neural vulnerability during adolescence remains uncertain. To address this question, we induced a transient period of hearing loss (HL) spanning adolescence in the gerbil, confirmed by assessment of circulating sex hormones, and asked whether behavioral and neural deficits are diminished. Wireless recordings were obtained from auditory cortex neurons during perceptual task performance, and within-session behavioral and neural sensitivity were compared. We found that a transient period of adolescent HL caused a significant perceptual deficit (i.e., amplitude modulation detection thresholds) that could be attributed to degraded auditory cortex processing, as confirmed with both single neuron and population-level analyses. To determine whether degraded auditory cortex encoding was attributable to an intrinsic change, we obtained auditory cortex brain slices from adolescent HL animals, and recorded synaptic and discharge properties from auditory cortex pyramidal neurons. There was a clear and novel phenotype, distinct from critical period HL: excitatory postsynaptic potential amplitudes were elevated in adolescent HL animals, whereas inhibitory postsynaptic potentials were unchanged. This is in contrast to critical period deprivation, where there are large changes to synaptic inhibition. Taken together, these results show that sensory perturbations suffered during adolescence can cause long-lasting behavioral deficits that originate, in part, with a dysfunctional cortical circuit.

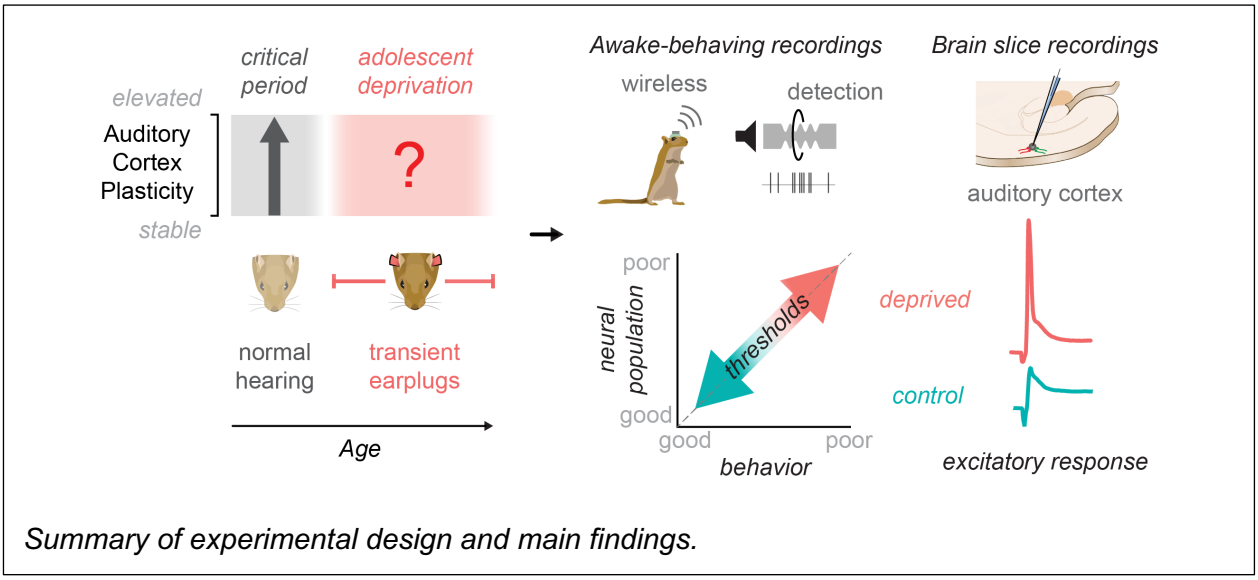

Summary of experimental design and main findings.

Main text / Introduction

The adolescent brain is distinguished by structural and functional changes that coincide with late-developing behavioral skills. In humans, synaptic pruning, myelination and cortical evoked-potentials each continue to mature well into the second or third decade of life (Sharma et al., 1997; Giedd et al., 1999; Moore and Guan, 2001; Bishop et al., 2007; Sussman et al., 2008; Pinto, 2010; Lebel and Beaulieu, 2011; Petanjek et al., 2011; Mahajan and McArthur, 2012b, 2012a; Shafer et al., 2015). Similarly, many behavioral skills are late to mature, including auditory perceptual learning (Huyck & Wright, 2011, 2013), temporal processing skills required for aural language (Banai et al., 2011; McMurray et al., 2018), face recognition (Carey et al., 1980; Germine et al., 2011), and fine motor control (Dayanidhi et al., 2013). Furthermore, the transition from childhood to adulthood is characterized by prolonged development of executive function (Selemon, 2013; Downes et al., 2017; Simmonds et al., 2017), emotion regulation (Guyer et al., 2008; Cohen Kadosh et al., 2013; Kadosh et al., 2013), and social skills (Blakemore, 2012). At the same time, adolescence is associated with risk factors, such as stress (Eiland and Romeo, 2013) or substance abuse (Davidson et al., 2015), and is a time during which many psychiatric disorders emerge (Paus et al., 2008). Here, we ask whether adolescent plasticity poses a risk for neural and behavioral development of sensory function, similar to postnatal critical periods (Hubel and Wiesel, 1970; Van der Loos and Woolsey, 1973; Knudsen et al., 1984b; Hensch, 2005; de Villers-Sidani et al., 2007; Popescu and Polley, 2010; Cheetham and Belluscio, 2014; Mowery et al., 2015).

There is broad agreement that, prior to sexual maturity, sensory deprivation can permanently disrupt central nervous system function when initiated during brief epochs, termed developmental critical periods (Hubel and Wiesel, 1970; Van der Loos and Woolsey, 1973; Knudsen et al., 1984b; Hensch, 2005; de Villers-Sidani et al., 2007; Popescu and Polley, 2010; Cheetham and Belluscio, 2014; Mowery et al., 2015). For example, a brief period of mild hearing loss (HL) can induce long-lasting changes to gerbil auditory cortex inhibitory synapses when it occurs before postnatal day (P) 19, but not after (Mowery et al., 2015, 2017). Furthermore, a similar period of HL induces perceptual deficits (Caras and Sanes, 2015), which can be rescued by restoring synaptic inhibition (Mowery et al., 2019). A perceptual deficit has also been reported for 5-year-old children with a history of transient HL (McKenna Benoit et al., 2018), in agreement with other human studies suggesting critical periods prior to sexual maturity (Sharma et al., 2002; Svirsky et al., 2004; Putzar et al., 2007, 2010).

While non-human research has focused on early critical periods, childhood HL can often emerge after birth (Lü et al., 2011; Barreira-Nielsen et al., 2016) and extend through adolescence (Niskar et al., 2001; Shargorodsky et al., 2010), resulting in more severe language deficits than those with brief HL (Yoshinaga-Itano et al., 1998; Tomblin et al., 2015). In fact, a majority of adolescents exhibit a mild-minimal high-frequency hearing loss that coincide with poorer speech perception in noise (Zadeh et al., 2019). Adolescents with HL are at risk for social isolation (Patel et al., 2020), and higher rates of psychiatric, depressive, or anxiety disorders (Theunissen et al., 2014). Thus, adolescence may be associated with greater vulnerability to even a transient period of auditory deprivation. To address this question, we asked whether a transient period of auditory deprivation, beginning after the auditory cortex (AC) critical period closes (Mowery et al., 2015, 2017, 2019) and extending throughout the period of sexual maturation, disrupts perceptual and neural auditory function. We found that a temporary period of adolescent HL led to impaired detection of amplitude modulations (AM), a foundational sound cue for aural communication including speech (Singh and Theunissen, 2003). These perceptual deficits were linked to poorer AC neuron encoding during task performance, and a change to AC synaptic properties distinct from that observed following critical period deprivation (Mowery et al., 2015, 2017, 2019). Taken together, our study suggests a sensitive period for sensory function during adolescent development.

Results

Transient sensory deprivation spans adolescence.

To determine whether auditory function is vulnerable during adolescence, we induced transient hearing loss (HL) at postnatal (P) day 23, after a well-defined AC critical period ends (Mowery et al., 2015). Normal hearing was restored (i.e., earplugs were removed) at P102, after the animals had passed through adolescence and reached sexual maturity (Figure 1A). To confirm the time course of sexual maturation, we tracked testosterone levels across development, both in normal hearing animals (n=12) and littermates with transient auditory deprivation during adolescence (n=14). Figure 1B shows serum testosterone levels for male (solid line) and female (dotted line) gerbils from P35 to P102. For males, testosterone levels were negligible at P35 (<0.2 ng/mL), rose sharply at P54 (2.42±0.8 ng/mL), and remained elevated thereafter. A two-way repeated measures ANOVA revealed a significant effect of age on testosterone levels ($F_{(4,39)}$ = 3.7, p=0.01), no effect of hearing loss ($F_{(1,39)}$ = 0.07, p=0.8), and no interaction between the two variables ($F_{(4,39)}$ = 0.56, p=0.7). For females, there was a small, transient rise in testosterone between P35 and P54, with no significant effect of hearing loss on testosterone levels ($F_{(1,38)}$ = 3.13, p=0.08). Therefore, the auditory deprivation between P23-102 likely spans the entirety of adolescence.

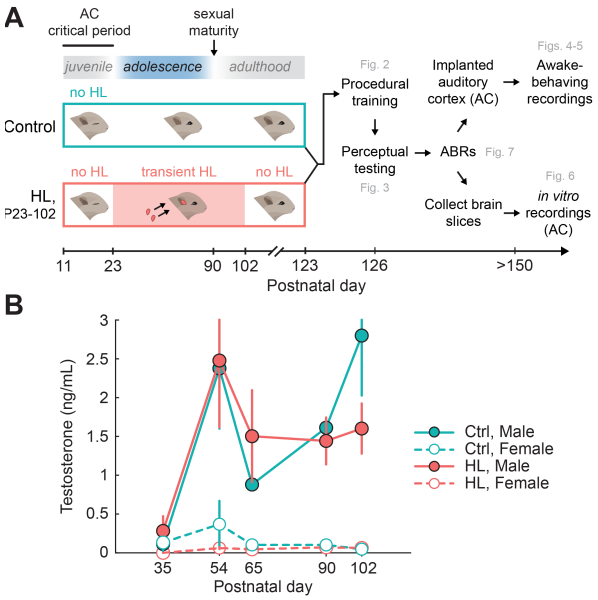

Figure 1. Transient sensory deprivation during adolescence. (**A**) Experimental timeline of manipulation and behavioral, physiological assessment. Gerbils either received transient hearing loss (HL; via bilateral earplugs) from postnatal (P) day 23, after the auditory cortex (AC) critical period ends, through P102, after sexual maturity (n=14) or no earplugs (littermate controls, n=12). Following earplug removal, animals recovered for 21 days prior to behavioral training and perceptual testing. Following behavioral assessment, auditory brainstem responses (ABRs) were collected in all animals, then were either chronically implanted in the AC and used for awake-behaving recordings (Ctrl: n=7; HL: n=9), or had brain slices collected for *in vitro* AC recordings (Ctrl: n=5; HL: n=5). (**B**) Serum testosterone levels across age for male (solid line) and female (dotted line) gerbils. The auditory deprivation induced spanned the entire time course of sexual maturation (estradiol not shown).

Adolescent hearing loss did not alter procedural learning.

Following transient HL and earplug removal at P102, gerbils recovered for 21 days prior to behavioral training on the amplitude modulation (AM) depth detection task (Figure 2A). Control and adolescent HL animals learned the AM detection task procedure at a similar rate (Figure 2B).

A two-way mixed-model ANOVA revealed a significant effect of trial number on performance ($F_{(74,1776)}$ = 19.8, p<0.0001), but no effect of earplug experience ($F_{(1,24)}$ = 0.2685, p = 0.61), and no interaction between the two variables ($F_{(74, 1776)}$ = 1.18, p = 0.1413). Thus, normal hearing controls and adolescent HL animals required a comparable number of Warn trials to reach the criterion for training performance (d' ≥ 1.5; Figure 2C). A one-way ANOVA revealed that the HL manipulation had no effect on the number of trials required to reach criterion during training ($t_{(24)}$ = -0.55; p = 0.59). In addition, the HL manipulation had no effect on the average d' achieved during the last 20 trials of procedural training (one-way ANOVA: $t_{(24)}$ = -0.23; p = 0.82; Figure 2D). Therefore, the two groups were equally proficient at task performance prior to psychometric testing.

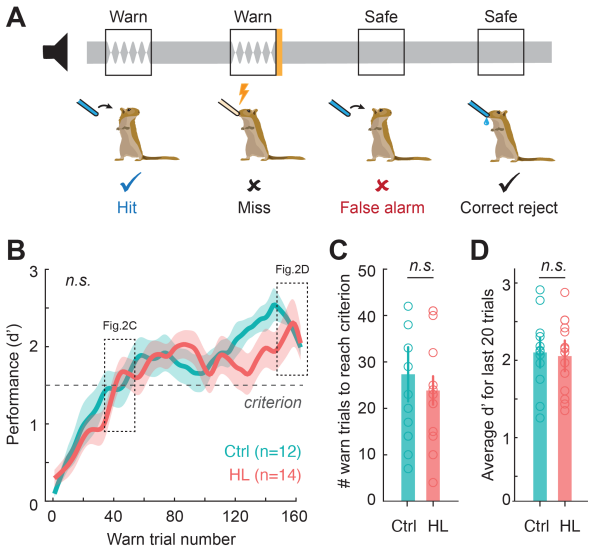

Figure 2. Hearing loss (HL) during adolescence did not alter procedural training performance in adulthood. (**A**) Schematic of the amplitude modulation (AM) detection task. Animals were trained to drink from a water spout in the presence of continuous broadband noise (Safe trials; classified as a "correct reject") and to cease drinking when the noise transitioned to a modulated "Warn" signal (0 dB relative to 100% AM noise; 5 Hz rate; classified as a "Hit"). Failure to withdraw from the spout during Warn trials (classified as a "Miss") resulted in a mild aversive shock. Withdrawing from the spout during Safe trials is classified as a "False Alarm". Behavioral performance is quantified by utilizing the signal detection metric, d'. (**B**) Procedural training sessions (3-4 separate sessions) were combined to compute behavioral performance (d') as a function of warn trial number using a 5-trial sliding window. Dotted line boxes correspond to data shown in C, D. Data are depicted as the mean ± SEM. (**C**) Number of warn trials to reach performance criterion (d'≥1.5; see horizontal line in **B**) for control (Ctrl) and HL-reared animals. (**D**) Average d' for the last 20 trials of procedural training for each group.

Adolescent hearing loss impaired amplitude modulation detection.

AM depth detection thresholds were assessed over 10 separate days of psychometric testing. Figure 3A shows psychometric functions on the first day of perceptual testing for normal-hearing animals (n=12) and those that experienced adolescent HL (n=14). HL animals displayed significantly poorer AM detection thresholds on the first day of testing (Ctrl: -11±0.5, HL: -8±0.7 dB re: 100% AM; $t_{(24)}$ = 2.98, p = 0.007; Figure 3B). The AM detection deficit did not resolve with perceptual learning (Sarro and Sanes, 2010, 2011; Fitzgerald and Wright, 2011; Caras and Sanes, 2015, 2017, 2019) over 10 consecutive sessions. In fact, adolescent HL animals displayed poorer AM detection thresholds across all testing days, even though both groups exhibited

perceptual learning (*initial*: HL: -8 dB; Ctl: -11 dB re: 100% AM; *final*: HL: -13 dB; Ctl: -16 dB re: 100% AM; Figure 3B). An analysis of covariance (ANCOVA; hearing status × log[test day]) revealed a significant effect of task experience ($F_{(1,206)}$ = 58.1, p<0.0001), such that AM detection thresholds decreased by 5 dB (re: 100% AM depth) per log(test day). There was no significant interaction between log(test day) and hearing status ($F_{(1,206)}$ = 0.72, p=0.4), but there was a significant effect of HL alone ($F_{(1,206)}$ = 53.2, p<0.0001) with AM detection thresholds 2.9 dB higher than controls across all testing days.

Elevated detection thresholds could be attributed to poorer hit rates (i.e., fewer correct responses to AM Warn trials) and/or elevated false alarm (FA) rates (i.e., incorrectly withdrawing from spout during Safe trials). Here, we find that FA rates consistently remain very low (< 0.06) across all testing sessions for both control and HL animals (grand average across testing sessions, Ctrl: 0.05; HL: 0.06; FA data not shown). An ANCOVA reveals no significant effect of testing day on FA rate ($F_{(1,254)}$ = 0.01, p=0.92), and no effect of HL ($F_{(1,254)}$ = 1.15, p=0.28). Therefore, the elevated detection thresholds in adolescent HL animals are due to poorer hit rates during AM Warn trials (Hit rate data not shown).

To determine whether adolescent HL influenced the magnitude of perceptual learning, we plotted the initial and the final AM threshold for each individual animal (Figure 3C). For animals with comparable starting thresholds (see dotted rectangle), those that experienced adolescent HL displayed smaller improvements than controls. To determine whether there was a significant difference in perceptual learning, we plotted perceptual improvement across the 10 testing days (i.e., initial threshold – final threshold) as a function of each animal's initial detection thresholds (Figure 3D). The gray rectangle highlights animals with comparable starting thresholds, and illustrates that adolescent HL animals displayed smaller improvement. The slopes of the linear regression fits to each group were not significantly different from one another (ANCOVA: $F_{(1,21)}$ = 0.07, p=0.8), but the adolescent HL curve had a significantly smaller y-axis intercept parameter (p<0.0001), showing that adolescent HL impaired perceptual learning.

Chronic stress during adolescence can have adverse effects on central nervous system structure and function (Isgor et al., 2004). To determine whether the perceptual deficits that we observed were due, in part, to elevated stress associated with earplugs, we obtained cortisol levels in each animal (Supplemental Figure 1) at five timepoints across development (P35, P55, P65, P90, and P102). We found no significant differences in cortisol levels between normal-hearing and

adolescent HL animals at any of the ages tested (Supplemental Figure 1A). In addition, we found no significant correlations between cortisol level at any developmental age with perceptual performance on the first day of testing (Pearson's r = -0.4 – 0.3; p-values of linear regression = -0.2-0.7), validating that the deficits observed were not due to elevated early life stress (Supplemental Figure 1B).

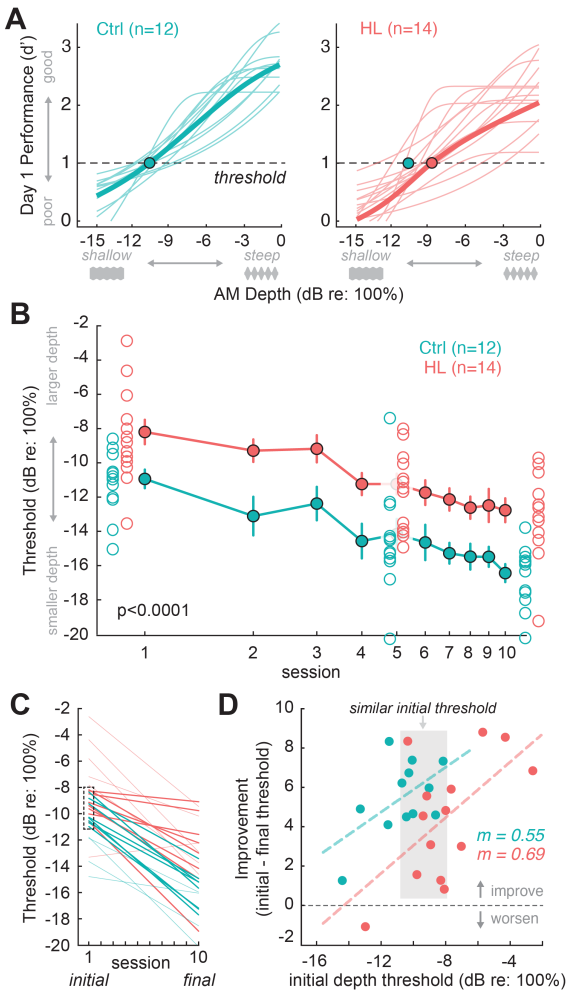

Figure 3. Transient hearing loss during adolescence impairs amplitude modulation (AM) depth detection in adulthood. (**A**) Psychometric functions on the first day of perceptual testing for control (Ctrl, n=12) and hearing loss (HL, n=14) animals. Threshold was defined as the depth at which d'=1 (dotted line). AM depths are presented on a dB scale (re: 100% depth), where 0 dB corresponds to 100% modulation, and decreasing values indicate smaller depths (e.g., see grey depth stimuli visualized below x-axes. Circle indicates the average group detection threshold. (**B**) HL animals display significantly poorer AM detection thresholds than controls on the first day of testing (Ctrl: -11±0.5, HL: -8±0.7 dB re: 100%; p=0.007). The AM detection deficit for HL animals persisted across 10 consecutive testing days. An analysis of covariance (ANCOVA) revealed the effect of HL alone to be significant (p<0.0001). (**C**) AM detection threshold for the first and last perceptual testing day for each individual animal. Bold lines indicate the animals that began with a similar initial threshold (see dotted rectangle). (**D**) Perceptual improvement (initial subtracted from final threshold) as a function of initial threshold. Values above the dotted line indicate an improvement in thresholds, whereas values below indicate a worsening of thresholds. The shaded area corresponds to animals with similar initial starting thresholds as indicated in (**C**). Dotted lines indicate fitted linear regressions (R^2=0.3-34). The slopes (m) of the regression fits were not significantly different from one another (p=0.8), while the y-axis intercepts were significantly different indicating the average amount of improvement was lower in adolescent-HL animals (p<0.0001).

<u>Diminished auditory cortex (AC) neuron detection thresholds during task performance in adolescent HL animals.</u>

Since perceptual deficits persisted long after peripheral input was restored, we asked whether it could be attributed to impaired auditory cortex (AC) encoding. A subset of behaviorally-tested gerbils (Ctrl: n=7; HL: n=9) were implanted with chronic 64 channel silicone electrode arrays in

the AC, and wireless neural recordings were collected as they performed the AM detection task (Figure 4A-B). We recorded from a total of 2,183 multi- and single-cortical units (Ctrl: n=846; HL: n=1337). Since individual sensory neurons have been shown to be predictive of behavior in perceptual discrimination (Pitkow et al., 2015) and detection tasks (Caras and Sanes, 2017), we opted to first examine detection thresholds for individual auditory cortical neurons. Multi- and single-units were selected for further analysis if they met the criteria for AM responsiveness (see Methods). We found 265 AM responsive units from control animals (multi-units: n=188; single-units: n=77) and 216 AM responsive units from adolescent HL animals (multi-units: n=154; single-units: n=62). The relatively low yield of AM responsive units included in the analysis allowed us to determine whether sensory encoding of AM can be explained by the sparse coding of a small subset of neurons and whether those neurons drive perceptual ability. Figure 4C shows raster plots and corresponding post-stimulus time histograms (PSTHs) for two example single units collected from a control and a adolescent HL animal. The plots display neural responses to unmodulated noise (Safe signal; *bottom panel*) and to a range of AM depths (Warn signal), from steeply modulated (-6 dB re: 100%; *top panel*) to shallow modulations (-18 dB re: 100%). Both example neurons display an increase in firing rate activity for modulated trials compared to unmodulated trials. In addition, firing rate increases with larger AM depths (Supplemental Figure 2A).

To determine whether adolescent HL alters AM detection thresholds, the firing rate of multi- and single-units that met the criteria for AM responsivity were transformed into d' values (see Methods). Neural d' was plotted as a function of AM depth and fit with a logistic function to generate neurometric functions for each cell. Figure 4D,E shows neurometric functions for a population of single units from control and HL animals. Similar to psychometric functions, neural detection thresholds were defined as the depth at which the neurometric fit crossed a *d'=1*. AC neurons from HL animals displayed significantly poorer thresholds, as compared to control neurons (Ctrl: -8.01±0.5; HL: -5.65±0.5 dB re: 100%; Figure 4F). A one-way ANOVA reveals a significant effect of HL on single unit neural thresholds ($F_{(1,128)}$ = 12.1, p = 0.0007). We find a similar effect of adolescent HL when we include multi-unit neural thresholds (Ctrl: -7.13±0.3; HL: 5.7±0.2 dB re: 100%; $F_{(1,451)}$ = 19.6, p < 0.001; Supplemental Figure 2F). Though only the "best" neurons were included in the analysis (i.e., met strict criteria for AM-responsivity), the AC neurons from adolescent HL animals still display poorer neural detection to AM.

Poorer AC neuron detection thresholds could be attributed to alterations in basic response

properties to AM depth stimuli. We find no effect of HL on overall firing rate of single-units (two-way mixed-model ANOVA: $F_{(1,135)}$ = 3.383, p = 0.07), though there is a significant effect of AM depth on firing rate ($F_{(1,135)}$ = 5.643, p=0.02) and no interaction between the two variables ($F_{(1, 135)}$ = 2.013, p = 0.16; Supplemental Figure 2D). However, we found that AC neurons from HL animals displayed weaker temporal coding of AM stimuli. We quantified how well single-unit neurons phase-locked to the AM stimulus by computing the vector strength (VS) at each AM depth (Supplemental Figure 2E) and find that AC neurons from HL animals displayed significantly lower VS values at each depth compared to control neurons (two-way mixed-model ANOVA: $F_{(1,135)}$ = 5.26, p = 0.023).

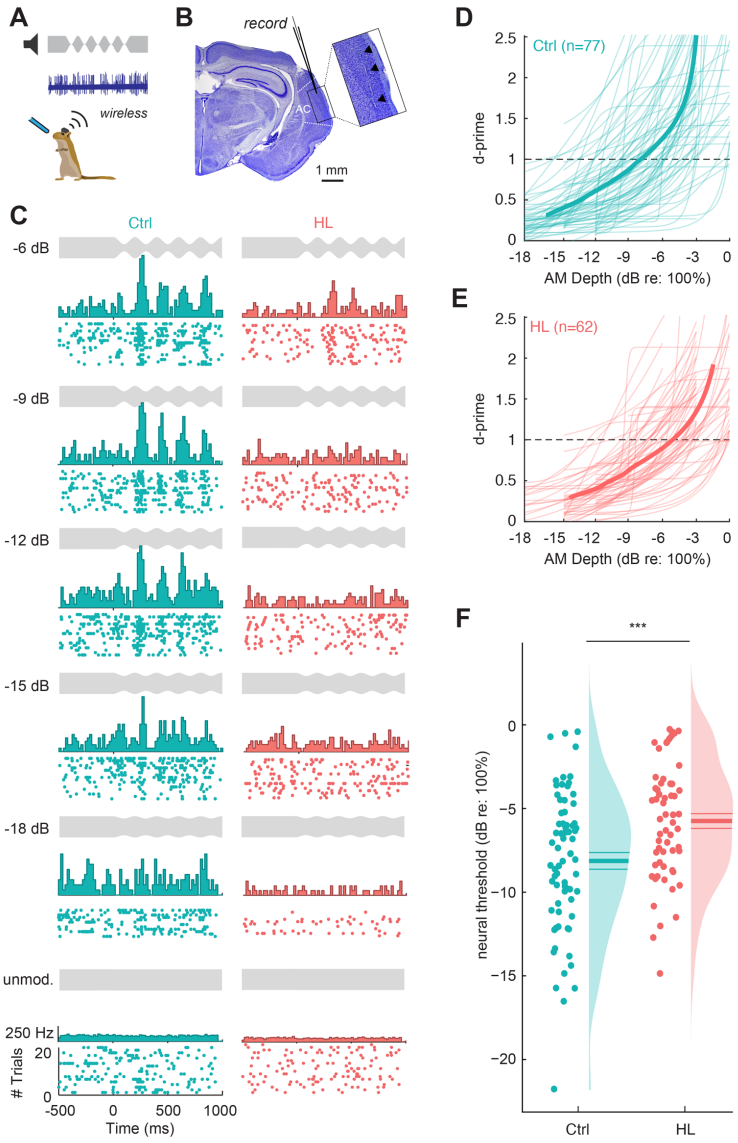

Figure 4. Single-unit analysis reveals poorer neural detection thresholds in the auditory cortex. (**A**) Chronic 64 channel electrode arrays were implanted into the auditory cortex (AC) of a subset of control (n=7) and HL (n=9) animals, and wireless neural recordings were collected as the performed the AM depth detection task. (**B**) Representative Nissl-stained coronal section from one implanted animal. Inset shows electrode track through primary AC (see arrows). (**C**) Raster plots with poststimulus time histograms are shown for two example single units from a control (left panel; Subject ID F276484) and HL (right panel; Subject ID M277481) animal. Plots are arranged in order from larger AM depths (top) to smaller depths (towards bottom; see depth stimulus in grey for reference). (**D, E**) The firing rate of single units that met the criteria for AM sensitivity were transformed into d' values (see Methods). Neural d' values were fit with a logistic function and plotted as a function of AM depth for a population of control (n=77) and HL (n=62) single units. Neural thresholds were defined as the AM depth at which the fit crossed d'=1. (**F**) Neural thresholds are plotted for control and HL animals. Individual thresholds are shown (circles), along with a half-violin plot indicating the probability density function. Horizontal lines indicate the mean±SEM. Single units from HL animals exhibit poorer neural depth thresholds than control single units (p = 0.0007).

Next, we explored whether detection thresholds for the sparse population of individual AC neurons aligned with perceptual performance. When we plot the behavioral threshold as a function of neural threshold, we find a positive correlation for both control and HL animals (Ctrl: Pearson's *r*: 0.36, p=0.06; HL: *r*: 0.58, p=0.0006; Supplemental Figure 3). This suggests that the neural AM detection thresholds for individual units can explain behavioral performance, but in general underestimates perceptual d' values. It is therefore likely that animals use more than the information provided by the most sensitive cortical neurons, leading us to explore whether AM detection performance can be better explained by population-level activity.

An auditory cortex population decoder can explain hearing loss-related behavioral deficits.

To determine whether AC population encoding could account for perceptual performance on the AM detection task, we used a previously described procedure (Yao and Sanes, 2018) to construct linear classifiers using support vector machines (SVM) (see Methods). Briefly, AM detection was calculated across our AC neuron population with a linear population readout scheme. The population linear classifiers were trained to decode responses from a proportion of trials to each individual Warn (AM) versus Safe (unmodulated) signal (Figure 5A). Cross-validated classification performance metrics included the proportion of correctly classified Warn trials ("Hits") and misclassified Safe trials ("False Alarms"). Similar to the psychometric and individual unit neurometric analyses, we converted population decoder performance metrics into d' values.

We applied the population decoder to the data in two ways. First, we assessed decoder performance for single- and multi-units within a behavioral session (i.e., within-session analysis, Figure 5B,C), and second, we assessed decoder performance for single units pooled across all behavioral sessions (Figure 5D). For the within-session analysis, we included sessions that had a minimum of 8 trials per depth recorded from a minimum of 10 multi- and/or single units. Figure 5B shows the population decoder results for an example session from a control and an adolescent HL animal. Similar to the psychometric functions and neurometric data collected for individual single units, the neural d' values are fit with a sigmoid to calculate neural threshold (where the fit crosses d'=1). Here, the neural thresholds for the example sessions show close alignment with behavioral threshold (vertical bars). When we compared behavioral threshold as a function of neural population threshold for all sessions that meet our criteria (Ctrl: 20 sessions; HL: 34 sessions), we found a strong correlation between behavioral and neural performance (Ctrl: Pearson's *r*: 0.58, p=0.008; HL: *r*: 0.44, p=0.01; Both groups combined: *r*: 0.6, p<0.001; Figure 5C).

Next, we assessed population decoder performance for single units pooled across behavioral sessions. Units were included in the decoder if behavioral sessions had a minimum number of 8 trials per depth. We opted to restrict the range of depths to -6 to -18 dB re: 100% for both control and HL groups to ensure neurons contributed equally to each depth for both groups. Figure 5D shows the results of the decoder for a population of single units pooled across 85 behavioral sessions (Ctrl: n=34 sessions; HL: 51 sessions) for control and adolescent HL animals (Ctrl: n=5 animals; HL: n=8 animals). Neural thresholds measured from population decoder performance was poorer for single units from adolescent HL animals as compared to control animals (Ctrl: ≤ -18 dB; HL: -11 dB re: 100%). Furthermore, the neural thresholds measured from population decoder performance closely aligned with perceptual thresholds.

In summary, we find that at the population-level, auditory cortical neurons from adolescent HL animals displayed poorer AM detection thresholds that were closely associated with psychometric performance. This indicates that both individual (Figure 4F) and population-level (Figure 5C,D) activity of AC single units reflect the HL-related AM detection deficits (Figure 3), though with more accuracy at the population-level. Overall, despite over ~8 weeks of normal audibility following transient adolescent HL, both the neural and behavioral deficit persisted in post-adolescent animals.

299

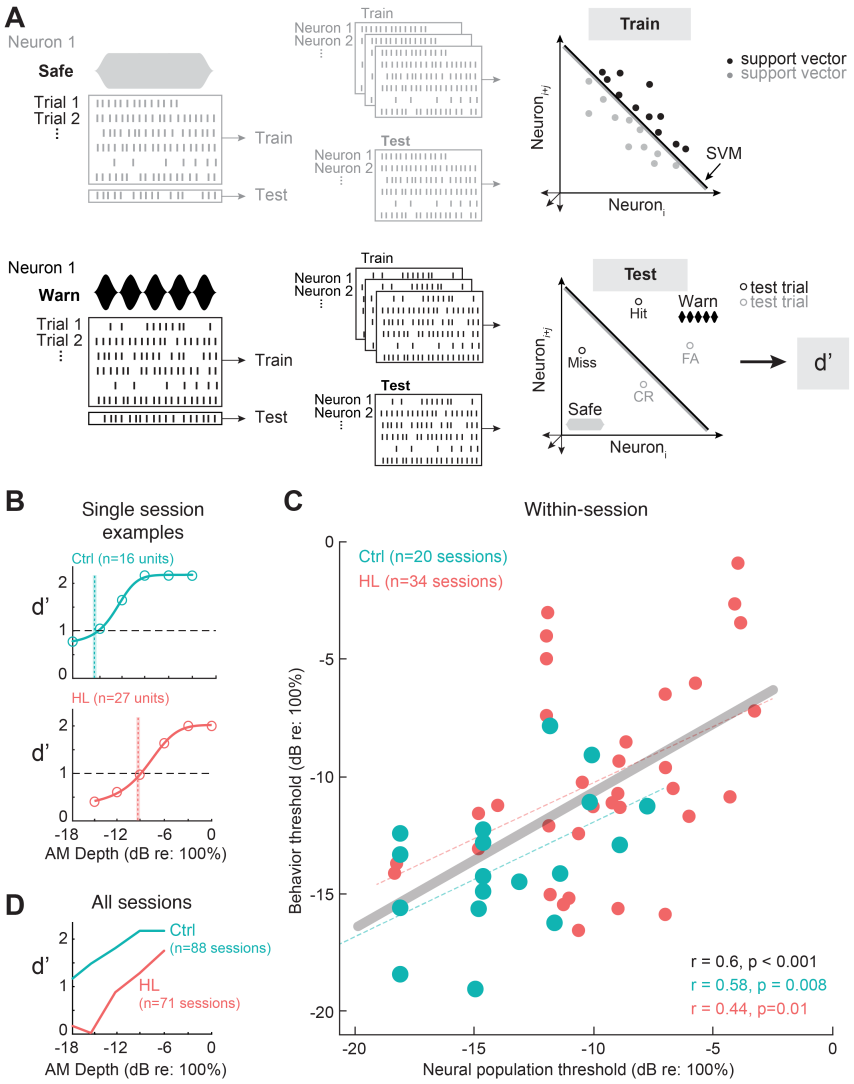

Figure 5. AC population decoder analysis can explain hearing-loss related behavioral deficits. (**A**) Schematic of AC population AM depth encoding with a linear population readout procedure. Hypothetical population responses for individual trials of a Safe (gray; unmodulated) and Warn (black; modulated) stimulus. Spikes were counted across the entire stimulus duration (1 sec) such that spike firing responses from *N* neurons to *T* trials of *S* stimuli ("Warn" and "Safe") formed a population "response vector". A proportion of trials ("leave-one-out" procedure) from each neuron were randomly sampled (without replacement) and fitted to a linear hyperplane that was determined by a support vector machine (SVM) procedure ("train" set). Symbols represent "support vectors", which are points used to create the linear boundary. Cross-validated classification performance was assessed on the remaining trials ("test" set). Performance metrics included the proportion of correctly classified Warn trials ("Hits") and misclassified Safe trials ("False Alarms"). Similar to the psychometric and individual unit neurometric analyses, we converted population decoder performance metrics into d' values. This procedure was conducted across 500 iterations with a new randomly drawn train and test set for each iteration. (**B**) Population decoder performance (d') for two example individual recording sessions as a function of AM depth from Ctrl and HL neuron populations. Neural d-prime values were fit with a logistic function (solid line), and threshold is defined as the AM depth where the fit crosses d'=1. Sample size indicates the number of single and/or multi-units included within that session. Shaded vertical bars indicate the behavioral threshold for that session. (**C**) Within-session correlations of behavioral threshold plotted as a function of multi-and single-unit population thresholds for that session. Dotted lines indicate the fitted linear regression for Ctrl and HL thresholds, and the solid line indicates the linear regresssion for both groups combined (grey). Pearson's *r* and statistical significance of each fit are noted in the bottom right corner of each plot. Behavioral sessions were included if they had at least 10 single and/or multi-units for the decoder analysis. (**D**) Average population decoder performance as a function of AM depth from Ctrl and HL single unit populations pooled across recording sessions.

Adolescent hearing loss induced long-lasting changes to auditory cortex excitatory synapses.

Transient adolescent HL induced persistent perceptual deficits that were correlated with diminished AC neuron sensitivity, but this effect could have been inherited from lower auditory centers. To test whether poorer neural encoding could be attributed, in part, to the AC, we obtained current clamp recordings in AC thalamocortical brain slices from a subset of behaviorally-tested animals (Ctrl: n=5; HL: n=5).

We first recorded electrical stimulus-evoked inhibitory postsynaptic potentials (IPSPs) from L2/3 pyramidal cells (Ctrl: n=16; HL: n=16) in the presence of ionotropic glutamate receptor antagonists (AP-5; DNQX; Figure 6A,B). Transient adolescent HL did not alter short-latency (putative $GABA_A$) IPSP amplitude (one-way ANOVA: $F_{(1,30)} = 0.31$, $p = 0.584$; Figure 6C), or long-latency (putative $GABA_B$) IPSP amplitude ($F_{(1,30)} = 0.76$, $p = 0.39$; Figure 6D). Total IPSP duration was also unaffected by HL ($F_{(1,30)} = 2.76$, $p = 0.11$; Figure 6E).

We next recorded electrically-evoked excitatory postsynaptic potentials (EPSPs) from L2/3 pyramidal cells (Ctrl: n=16; HL: n=16) at a holding potential of -80 mV (Figure 6F,G). As shown in Figure 6H, neurons from HL animals required a much lower stimulus current to evoke an action potential (AP). Therefore, a higher proportion of cells from adolescent HL animals fires APs at lower afferent stimulation levels than control cells (Figure 6I), with the average afferent stimulus required to elicit APs of 0.4 mA compared to 0.9 mA in control cells. A two-way mixed model ANOVA revealed a significant effect of HL on EPSP maximum amplitude ($F_{(1,30)} = 5.74$, $p = .0231$), a significant effect of stimulus level ($F_{(9,22)} = 37.52$, $p<.0001$), and no interaction between the two variables ($F_{(9,22)} = 0.853$, $p = 0.58$).Finally, we recorded L2/3 pyramidal cell firing rate in response to current injection (Ctrl: n=32; HL: n=31; Figure 6J,K). Adolescent HL did not alter maximum firing rate ($F_{(1,61)} = 0.649$, $p = .4274$; Figure 6L), or first spike latency ($F_{(1,21)} = 1.21$, $p=0.29$; Figure 6M).

In summary, we find that adolescent HL induces intrinsic and synaptic changes to cortical properties that are distinctly different than the changes observed with critical period HL (Mowery et al., 2015).

327

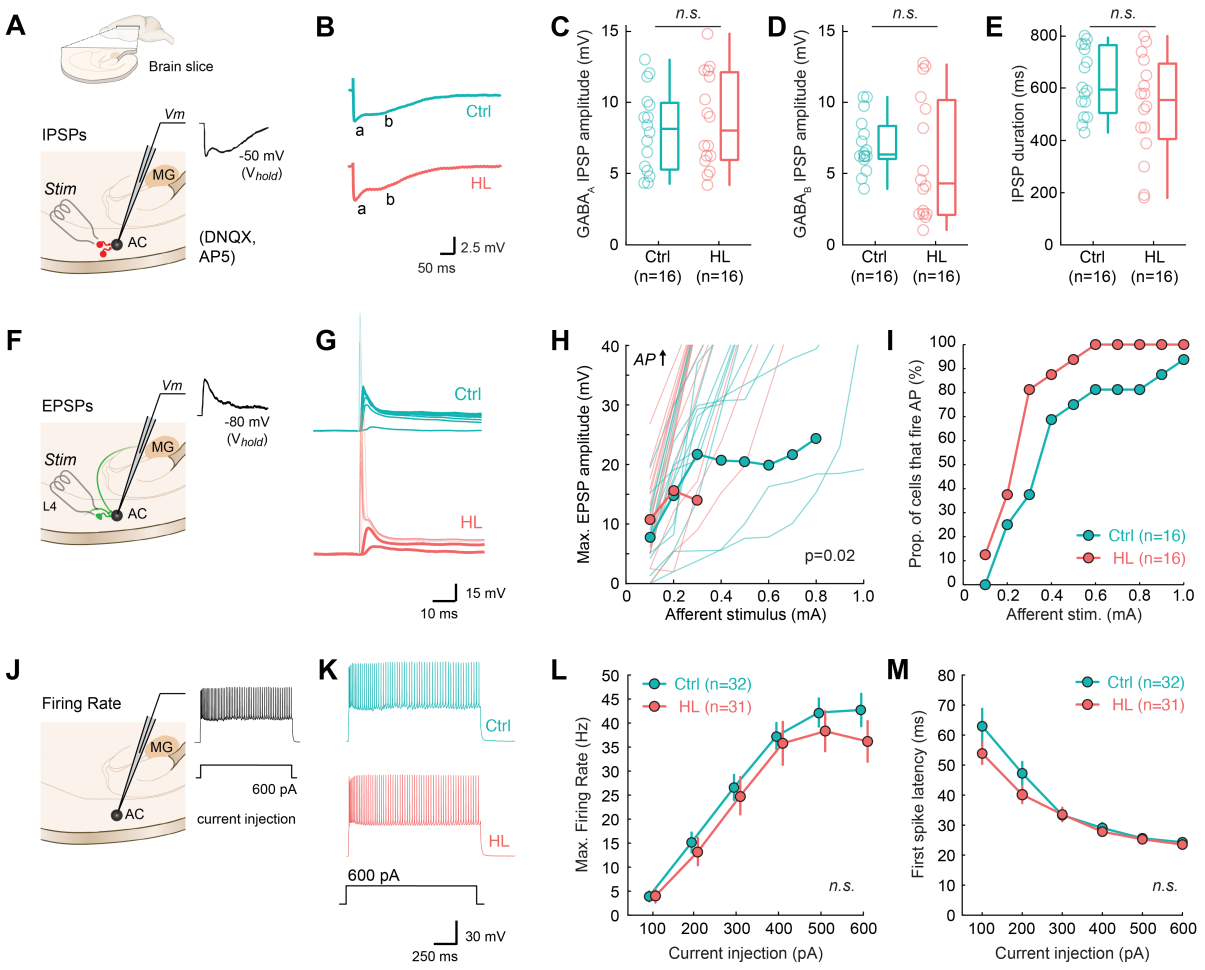

Figure 6. Hearing loss spanning adolescence induces long-lasting changes to auditory cortical properties. (**A**) Schematic of perihorizontal brain slices collected from control (n=5) and HL-reared animals (n=5; inset). Slices contain the auditory cortex (AC), where recordings from layer 2/3 pyramidal cells were made following electrical stimulation (Stim) of fast-spiking inhibitory interneurons to examine synaptic inhibition (IPSPs). Evoked IPSPs were collected in the presence of DNQX and AP-5 to isolate inhibitory potentials. (**B**) Example IPSP traces from control (Ctrl) and HL-reared (HL) cortical cells. Labels a, b indicate putative $GABA_A$ and $GABA_B$ components, respectively. (**C-E**) $GABA_A$ receptor-mediated IPSP amplitudes, $GABA_B$ receptor-mediated IPSP amplitudes, and overall IPSP duration are not altered by adolescent HL. (**F**) Recordings from layer 2/3 pyramidal cells were made following electrical stimulation of local L4 excitatory interneurons to examine synaptic excitation (EPSPs). (**G**) Example evoked potentials in response to increasing afferent stimulus levels (0.1-1 mA). EPSP traces are in bold and action potentials (APs) elicited are transparent. Stimulus artifact was removed for clarity. (**H**) Max amplitudes were determined from EPSP waveforms for each stimulation level plotted as input-output functions. Transparent lines indicate individual data, and bold lines with circles indicate mean±SEM if n≥3. (**I**) Proportion of cells that fire APs as a function of afferent stimulation level (mA) for each group. Adolescent HL led to a higher proportion of cells firing APs at lower afferent stimulation levels compared to control cells. (**J**) The firing rate of AC cells were collected via current injection into the cell. (**K**) Example traces of current-evoked responses to a depolarizing current injection (600pA). (**L**) Input-output function for maximum firing rate in response to current injection steps (100-600pA). HL during adolescence did not significantly impact current-evoked firing rate. (**M**) First spike latency with increasing current injection (pA).

Behavioral and central AM processing deficits are unrelated to peripheral function.

One alternative explanation for the AM detection behavioral deficits is that a long duration of HL could induce changes to auditory peripheral structures at, or below, the level of the auditory brainstem. To explore this possibility, we collected auditory brainstem response (ABR) measurements from Control (n=12) and HL (n=13) animals after they completed psychometric testing (Figure 3), and prior to chronic electrode implantation and/or thalamocortical brain slice collection (e.g., see timeline in Figure 1A). Figure 7B shows ABR thresholds in response to a range of tone frequencies (0.5, 1, 2, 4, 5, 8, 16 kHz) for Control and HL animals (i.e., the ABR "audiogram"). The average tone ABR thresholds for HL animals were slightly elevated compared to controls (two-way mixed model ANOVA: $F_{(1,21)} = 8.98$, $p = 0.01$). To determine whether this was due to a residual conductive loss or was sensorineural in origin, we examined ABR amplitude input-output functions because subtle damage to auditory nerve synapses has been associated with shallower ABR input-output functions, even when ABR thresholds are normal (Liberman and Kujawa, 2017). Figure 7C shows 4 kHz wave I amplitude (μV) as a function of sound level (dB SPL) for two example ABRs from a control and HL animal. A linear regression was fit to each set of data points (Pearson's r>0.9) which gives rise to a slope value, indicating the wave I amplitude increment of change, or growth, with sound level (μV/dB). For these two examples, the slope is nearly identical (Ctrl: 0.011; HL: 0.012 μV/dB). When we examined all the data collected, we found no differences in the 4 kHz ABR amplitude wave I growth (μV/dB) between control animals (mean ± SEM: 0.0083±0.002 μV/dB) and HL animals (0.0085±0.002 μV/dB). A one-way ANOVA verifies that HL experience did not affect ABR amplitude growth ($F_{(1,23)} = 0.03$, $p = 0.87$).

Finally, if ABR thresholds were causally related to behavioral thresholds, then we would expect a correlation between them. Figure 7E plots individual behavioral thresholds as a function of 4 kHz ABR threshold for Control and adolescent HL animals. Fitted linear regressions displayed no correlation (Ctrl, Pearson's $r = -0.08$; HL, $r = 0.04$).

Taken together, Control and HL animals both exhibit comparable ABR wave I amplitude growth with sound level indicating that the auditory nerve fibers were not compromised following adolescent HL. Moreover, we found no relationship between tone ABR thresholds and behavioral performance, suggesting that the perceptual deficit we observed was due to central changes at the level of the auditory cortex, not peripheral changes at, or below, the level of the auditory brainstem.

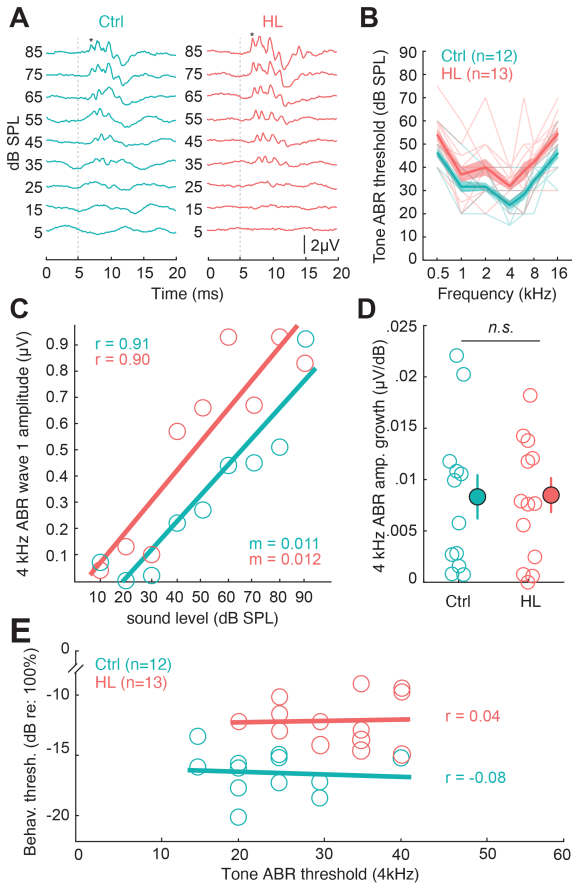

Figure 7. Control experiment: HL-related AM detection deficits are not due to status of auditory periphery. (**A**) Auditory brainstem response (ABR) waveforms in response to 4kHz tone pips for example control (Ctrl, Subject ID: M274129) and HL-reared animal (HL, Subject ID: M274131). Vertical dotted line indicates stimulus onset. Asterisk (*) indicates ABR wave 1. (**B**) Tone ABR Thresholds (mean±SEM) as a function of frequency (kHz). (**C**) 4kHz ABR wave 1 amplitude (μV) as a function of sound level (dB SPL) for two example Ctrl and HL animals. Solid line indicates linear fit; m indicates the slope of the fit. Pearson's *r* value for each regression are noted on the top left corner. (**D**) 4kHz ABR wave 1 amplitude growth is comparable between Ctrl and HL-reared animals. Amplitude growth values are calculated from the slope of the linear regression to wave 1 amplitude with sound level (i.e., in C). (**E**) Individual behavioral threshold as a function of ABR threshold at 4 kHz. Behavioral thresholds were from the final day of psychometric testing, closest to when the ABR was collected. Solid line indicates fitted linear regression. Horizontal linear fits indicate no correlation (Pearson's $r \leq 0.04$ for both groups) between tone ABR thresholds and behavioral thresholds.

361

362 <u>AM depth detection thresholds remain consistent with relevant sound levels.</u>

363 To further test the possibility that a residual conductive loss could contribute to AM detection
364 deficits, we determined how behavioral depth detection thresholds vary with sound level. If
365 thresholds do not vary across a large range of sound levels, then that would suggest a small
366 residual conductive loss could not explain the behavioral findings.

367

368 A group of normal hearing animals (n=4) were trained on the AM depth detection task (Figure
369 8A). After obtaining AM detection thresholds at the same sound level used for the experimental
370 groups (45 dB SPL; Figure 8B), the sound level was varied from 10-60 dB SPL across 24 testing
371 sessions, with at least 3 sessions per level (Figure 8C). Figure 8D shows depth detection
372 thresholds as a function of sound level for all animals. A one-way ANOVA revealed a significant
373 effect of sound level on detection thresholds ($F_{(7,87)} = 3.25$, $p = 0.004$), and a Tukey HSD *post hoc*
374 test for pairwise comparisons revealed 10 dB SPL was significantly different from all other levels

(p<0.0001), and 15 dB SPL was significantly different from 40 dB SPL (t = 3.21, p = 0.04), 45 dB SPL (t = 3.92, p = 0.004), and 60 dB SPL (t = 3.73, p = 0.008). All other sound levels were not significantly different from one another (p=0.3-1.0). To determine the level at which thresholds remained consistent with sound level, a 3-parameter exponential was fit to the data (dotted line in Figure 8D). We found that thresholds asymptote at -15.8 dB (re: 100% AM), which corresponds to 27 dB SPL. This indicates that depth detection thresholds remain stable for sound levels greater than 27 dB SPL, which is well below the sound level used in the behavioral and awake-behaving experiments (45-60 dB SPL). This suggests that even if an animal has a mild peripheral HL (<20 dB), behavioral detection thresholds would not be significantly impacted. This further supports the notion that the behavioral deficit we observed in animals after adolescent HL is due to central changes at the level of the AC, and not due to peripheral auditory mechanisms.

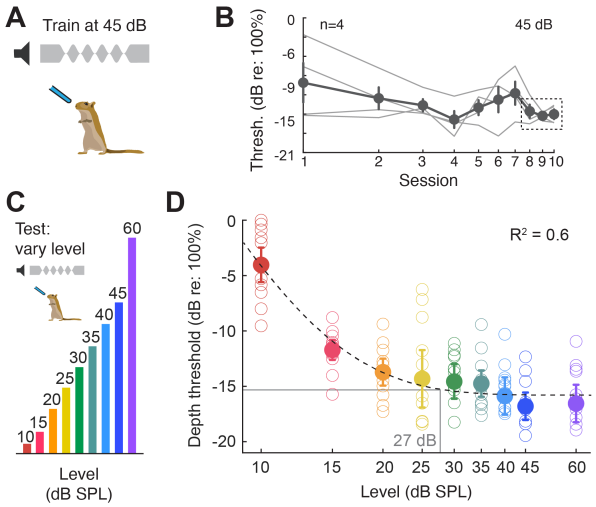

Figure 8. Control experiment: AM depth detection thresholds remain consistent with varying sound levels. (**A**) Animals (n=4) were trained on the AM depth detection task at 45 dB SPL. (**B**) Depth detection thresholds as a function of 10 testing days. Once detection thresholds stabilize (i.e., consistent for 3 consecutive sessions: dotted rectangle), then the sound level was varied from 10-60 dB SPL (**C**). (**D**) Behavioral AM depth detection thresholds across sound level (dB SPL). Open circles indicate individual performance (3 sessions per animal) and solid circles indicate the group mean (± SEM). A 3-parameter exponential was fit to the data (dotted line). Thresholds asymptote at -15.8 dB (re: 100% AM), which corresponds to 27 dB SPL. Therefore, depth detection thresholds remain consistent for sound levels greater than 27 dB SPL.

Discussion

The extent to which perceptual skills are influenced by adolescent sensory experience remains uncertain. Before sexual maturity, the influence of sensory experience is profound, and brief periods of diminished or augmented stimulation can permanently alter central nervous system function (Hubel and Wiesel, 1970; Van der Loos and Woolsey, 1973; Knudsen et al., 1984b; Hensch, 2005; de Villers-Sidani et al., 2007; Han et al., 2007; Zhou and Merzenich, 2009; Popescu and Polley, 2010; Christakis et al., 2012; Cheetham and Belluscio, 2014; Mowery et al., 2015). However, both CNS function and perception continue to mature after the onset of sexual maturation (Carey et al., 1980; Sharma et al., 1997; Giedd et al., 1999; Moore and Guan, 2001; Bishop et al., 2007; Sussman et al., 2008; Guyer et al., 2008; Pinto, 2010; Banai et al., 2011; Huyck and Wright, 2013; Lebel and Beaulieu, 2011; Petanjek et al., 2011; Germine et al., 2011; Huyck and Wright, 2011; Mahajan and McArthur, 2012b, 2012a; Kadosh et al., 2013; Selemon, 2013; Cohen Kadosh et al., 2013; Dayanidhi et al., 2013; Shafer et al., 2015; Simmonds et al., 2017; Downes et al., 2017; McMurray et al., 2018), suggesting that sensory plasticity could remain heightened during adolescence. Here, we report that a period of mild auditory deprivation during adolescence induced long-lasting perceptual deficits that could be explained by intrinsic changes to auditory cortex (AC) excitatory synapse function and degraded AC population encoding during task performance.

Comparison between juvenile and adolescent plasticity

Mammals display enhanced plasticity from early infancy through juvenile development, allowing for both positive and negative environmental influences. Foremost among these is the early influence of sensory experience: finite periods of monocular deprivation shortly after eye opening result in long-term visual acuity deficits that are closely associated with degraded cortical processing (Hubel and Wiesel, 1970). Early critical periods are found in humans: children born with dense cataracts exhibit long-term visual acuity deficits even after cataract removal (Lewis and Maurer, 2005; Jain et al., 2010) and, similarly, those born with profound hearing loss display a neonatal epoch during which cochlear prostheses provide maximal restoration of neural and behavioral performance (Sharma et al., 2002).

Adolescent plasticity displays some unique characteristics, as neural function and behavioral skills slowly transition to an adult phenotype (Sawyer et al., 2018). For example, there is a transient reduction in some forms of learning or memory. This includes slower rates of auditory

perceptual learning (Huyck and Wright, 2011; Caras and Sanes, 2019), reduced voice or face recognition (Mann et al., 1979; Carey et al., 1980), and diminished extinction learning (McCallum et al., 2010; Kim et al., 2011; Pattwell et al., 2012). There are also indications that adolescents are vulnerable to environmental factors. For instance, social experience during early adolescence is particularly important for the subsequent development of these skills (Burke et al., 2017). Rats that experience social isolation from a late juvenile to early adolescent age exhibit abnormal exploratory behavior when placed in a novel environment (Einon and Morgan, 1977), while social deprivation before or after this age range is not damaging. In addition, rats that experience chronic stress throughout adolescent development exhibit long lasting structural changes in the hippocampus that coincide with spatial navigation impairments (Isgor et al., 2004). Our results suggest that adolescent vulnerability noted above extends to skill learning. We found that transient adolescent HL led to significantly poorer perceptual learning of the auditory task (Figure 3D).

Effects of adolescent sensory deprivation

The current findings suggest that adolescent neural plasticity differs dramatically from that observed during the AC critical period. One novel outcome from this study is that critical period and adolescent HL induce similar behavioral deficits, but each are associated with unique synaptic mechanisms. Transient HL during the critical period (P11-23) causes reduced inhibitory synaptic strength and a decrease in membrane excitability in AC neurons (Kotak et al., 2005, 2008; Takesian et al., 2010, 2012; Mowery et al., 2015, 2019). In contrast, we found that transient HL spanning adolescence had no effect on synaptic inhibition or current-evoked firing rates. Rather, adolescent HL led to elevated excitatory postsynaptic potential amplitudes in AC pyramidal neurons (Figure 6). A second novel outcome is that adolescent HL leads to a significant deterioration of AC stimulus encoding during task performance (Figures 4 and 5), despite having no effect on neural discharge rate (Supplemental Figure 2). This is in marked contrast to critical period HL which causes a significant decrease of AC neuron firing rate (Rosen et al., 2012; Yao and Sanes, 2018). Taken together, these findings suggest that adolescent neural plasticity in response to sensory deprivation is mechanistically distinct from that observed during early critical periods.

A third novel finding is that the effects of adolescent HL are more persistent than those observed following brief HL during the AC critical period. For example, restoring normal auditory input at P17 in the gerbil, before closure of the AC critical period (P23), led to a near-complete recovery

of intrinsic cellular properties whereas restoring auditory input after the critical period ends (P23) led to persistent AC alterations (Mowery et al., 2015). A transient period of developmental HL can also cause perceptual deficits, though these often resolve gradually (Hall et al., 1995; Moore et al., 1999; Caras and Sanes, 2015; McKenna Benoit et al., 2018). Thus, we previously reported that brief HL during an AC critical period (P11-23) led to a perceptual deficit, while the same manipulation had no effect when initiated after the critical period closed (P23) (Caras and Sanes, 2015). In contrast, our current study found significant and persistent perceptual impairments following HL that was induced at the same postnatal age, P23. This suggests that auditory function is susceptible to deprivation after the AC critical period, but only if the deprivation persists throughout adolescence. In fact, we found that adolescent HL induced longer lasting perceptual deficits than those observed with critical period HL. Following adolescent HL, neural and behavioral deficits were still present for over ~8 weeks following restoration of normal auditory input, whereas the critical period-induced perceptual deficits largely resolved over the same recovery period (Caras and Sanes, 2015).

Alternative explanations for the effect of auditory deprivation

We find that adolescent HL induces intrinsic changes to AC neurons that contributes to poorer AM detection thresholds long after normal hearing is restored. However, it is also possible that the long duration of the hearing deprivation compromised peripheral auditory structures, resulting in decreased audibility. For instance, subtle damage to auditory nerve synapses is evidenced by shallower ABR input-output functions even with normal ABR thresholds (Furman et al., 2013; Liberman and Kujawa, 2017). However, our ABR measurements reveal no significant differences in ABR wave I rate of amplitude growth with sound level (Figure 7D), indicating intact auditory nerve function. Although we find a modest difference in tone-ABR thresholds following adolescent HL, this does not account for poorer perceptual performance (Figure 7E). Furthermore, we find that AM detection thresholds are largely independent of sound level (above 27 dB), consistent with other assessments of AM depth sensitivity (Viemeister, 1979). This suggests that even if an animal has a mild residual peripheral HL, AM detection thresholds would not be significantly impacted as the sound level used in the behavioral and awake-behaving experiments far exceed the potential HL. Recently, Ye et al. (2021) report that a moderate form of permanent peripheral HL (~35-40 dB conductive loss) does not appreciably alter frequency tuning in the cochlea, and attribute associated perceptual dysfunction to central, and not peripheral, auditory mechanisms.

A second possibility is that the adolescence, itself, was disrupted by the manipulation. To directly identify the period of adolescence in the gerbil, and confirm that it was not altered by our

manipulation, we measured testosterone levels from each subject throughout development. We identified a developmental window during which testosterone levels increased, and found it to be identical between normal hearing and earplugged animals, and consistent with a previous report (Pinto-Fochi et al., 2016). Since female gerbils generally reach sexual maturity concurrently with or prior to their male counterparts (Norris and Adams, 1974), it is plausible that the HL manipulation spanned sexual development for both sexes. Therefore, a change to adolescent maturation was unlikely to account for our results. It was also possible that the earplug manipulation caused chronic stress during adolescence which adversely effects the CNS (Isgor et al., 2004). However, cortisol levels did not differ between treatment groups (Supplemental Figure 1), and displayed no correlation with perceptual performance. Therefore, chronic stress was unlikely to explain our findings.

The timing and duration of developmental hearing loss

Sensory manipulations that target adolescence are somewhat uncommon. In the auditory system, manipulations have primarily targeted either early development, shortly after hearing onset, or adults, well after sexual maturity. For instance, transient HL (i.e., using earplugs, ear canal ligation, or poloxamer hydrogel) has been induced at hearing onset in the guinea pig (Clements and Kelly, 1978), gerbil (Caras and Sanes, 2015; Mowery et al., 2015, 2017, 2019; Green et al., 2017), barn owl (Knudsen et al., 1982, 1984b, 1984a; Knudsen, 1983, 1985; Mogdans and Knudsen, 1992, 1993), ferret (Moore et al., 1999; Keating et al., 2013, 2015a), rat (Popescu and Polley, 2010), and mouse (Polley et al., 2013; Zhuang et al., 2017). Permanent forms of mild-moderate HL (i.e., conductive HL through ossicle disruption or surgical intervention of the ear canal) have also been induced at hearing onset of a variety of species (gerbil: Xu et al., 2007; Rosen et al., 2012; Takesian et al., 2012; Buran et al., 2014a; Gay et al., 2014; Ihlefeld et al., 2016; von Trapp et al., 2017; Yao and Sanes, 2018; rat: Clopton and Silverman, 1977; Silverman and Clopton, 1977; mouse: Xu and Jen, 2001; cat: Moore and Irvine, 1981; Brugge et al., 1985).

The duration of developmental HL manipulations vary widely, as does its relationship to the age of sexual maturity. For instance, Polley et. al. (2013) induced a ~7 day auditory deprivation beginning at P12 in the mouse, a species that reaches sexual maturity around postnatal day 49 (Danneman et al., 2012). A similar duration of HL would represent a much smaller fraction of development for species with longer periods of adolescence (e.g., sexual maturity in the ferret is 4-6 months or ~1 year in the barn owl). Though the majority of transient HL studies focus on relatively brief deprivation early in development, there are a few that span the late juvenile through

adolescent period. A reversible HL was induced in barn owls beginning at posthatch day 28, approximately 20 days after hearing onset, and normal audibility was restored between days 120-213, prior to the age of sexual maturity at ~1 year (Knudsen et al., 1984a; Knudsen et al., 1985; Mogdans and Knudsen, 1992; Mogdans and Knudsen, 1993). Similarly, a transient HL was induced in the ferret at P24-25, just before hearing onset, and audibility was restored at P126 or P213, after sexual maturity at ~P121-152 (Moore et al., 1999; Keating et al., 2013; Keating et al., 2015b). The relatively long duration developmental HL in both the barn owl and ferret studies induced long-lasting neural and behavioral deficits, similar to our current findings. However, none of the previously reported studies exclusively targeted adolescence after the critical period.

Our results are also consistent with clinical evidence that suggests longer durations of developmental HL can induce more harmful effects. Children with progressive, late-onset, or acquired HL (Smith et al., 2005) often pass newborn hearing screenings, leading to long periods of undetected HL. Those with an extended period of unresolved HL display more severe language deficits than those with a brief HL (Yoshinaga-Itano et al., 1998; Tomblin et al., 2015). Here, we find that a long duration HL that spans adolescence led to AC neural changes that are distinctive from critical-period plasticity during juvenile development. We conclude that the changes to AC synaptic excitability observed following adolescent HL contributes to the AC encoding deficits observed with the awake behaving neural recordings (Figures 4-5). Taken together, these results reveal that transient HL spanning adolescence permanently alters AC cellular properties, thereby diminishing sensory encoding of AM stimuli during the detection task, and explains the long-term auditory perceptual limitations observed in adolescent HL animals.

Methods

Experimental subjects

A total of 30 Mongolian gerbils (*Meriones unguiculatus,* 19 females, 11 males) were used in the study. Pups were weaned from commercial breeding pairs (Charles River Laboratories) at postnatal (P) day 30 and housed on a 12-hour light / 12-hour dark cycle with full access to food and water, unless otherwise noted. All procedures were approved by the Institutional Animal Care and Use Committee at New York University.

Hormone assessment

Estradiol, testosterone, and cortisol hormone levels were collected in developing gerbils through blood sample collection at five timepoints spanning development (P35, P55, P65, P90, and P102). Animals were briefly anesthetized with isoflurane/O2 and placed on a heating pad. The fur at the base of the tail was removed using a scalpel blade for greater visualization and access to the lateral tail vein. A small incision was made and the blood from the lateral tail vein was collected in Eppendorf vials (100-300µl). To reduce acute stress-induced changes to cortisol levels, all blood collection was obtained within 3 minutes of placing animals under anesthesia. Blood collection was also collected at the same time of the day for each animal at each testing age (early afternoon) to avoid circadian-related hormonal fluctuations. Blood samples were centrifuged (for 9 minutes, 8,000g) within 30 minutes to avoid hemolysis of the blood. After spinning, the serum component of the blood was extracted into a separate vial and stored in a -80° freezer until samples were ready to be processed.

Serum samples were shipped to the Endocrine Technologies Core (ETC) at the Oregon National Primate Research Center (ONPRC) for quantification of hormone levels. Serum concentrations of estradiol (E2), testosterone (T), and cortisol (F) were simultaneously measured by liquid chromatography-tandem triple quadrupole mass spectrometry (LC-MS/MS) using a previously established method(Bishop et al., 2019). Briefly, serum samples were combined with a mixture of deuterium-labeled internal standards for E2, T, and F. Steroids were extracted using supported liquid extraction (SLE) and analyzed on a Shimadzu Nexera-LCMS-8050 LC-MS/MS platform. 9-point calibration curves for each hormone were linear throughout the assay range (13 pg/ml – 26.67 ng/ml; R>0.99). The lower limit of quantitation for each hormone was 13 pg/ml. Intra-assay CVs were 15% for E2, 2.9% for T, and 3.8% for F. Serum testosterone and cortisol levels were successfully obtained using the LC-MS/MS approach; however, estradiol was not detected in any

of the serum samples indicating that the assay was not sensitive enough to determine estradiol levels (i.e., values were below the lowest calibration level and could not be quantified).

Transient auditory deprivation

Custom earplugs (BlueStik adhesive putty, super glue, and KwikSil silicone adhesive) were used to induce a reversible, transient hearing loss (HL). Earplugs provided a mild-moderate temporary HL, attenuating ~10-20 dB at frequencies ≤ 1 kHz and 30-50 dB at frequencies ≥2 kHz (Caras and Sanes, 2015). Gerbils either received bilateral earplugs from P23 (after the auditory cortex critical period) through P102 (after sexual maturity; n=14) or no earplugs (littermate controls, n=12). Animals were briefly placed under isoflurane anesthesia and the ear canal and tympanic membrane were visualized under a stereomicroscope (Olympus). A small adhesive putty "disk" was gently inserted into the ear canal and compressed into the bony portion of the canal. Care was taken to ensure that the earplug material did not go near the tympanic membrane. A small drop of super glue was placed onto the putty and allowed to fully dry before covering the earplug with a layer of KwikSil silicone adhesive. Earplugs were checked 1-2x daily and replaced as needed. Following earplug removal, the tympanic membrane was visualized (at the time of removal as well as post-mortem) to ensure the membrane was intact and free from debris. Littermate control animals also underwent daily handling and had comparable isoflurane exposure with similar manipulations of their pinna (i.e., used forceps to mimic earplug placement) as their earplugged counterparts. Animals were allowed to recover for 21 days prior to behavioral and physiological testing.

Behavioral training and testing

Behavioral apparatus

All behavioral experiments were performed in a sound-attenuating booth (Industrial Acoustics) and were observed through a closed-circuit video monitor (Logitech HD C270 Webcam). Animals were placed in a custom-made, acoustically-transparent plastic test cage with a stainless steel water spout positioned above a metal platform. Sound stimuli were delivered from a calibrated free-field speaker (DX25TG0504; Vifa) positioned 1 m above the test cage. Contact with the waterspout was assessed via infrared sensor (OP550 NPN Silicone phototransistor, Digikey) and emitter (940 nm; LTE-302, Digikey) housed within a custom apparatus encasing the waterspout. Acoustic stimuli, water reward delivery, experimental parameters, and data acquisition were controlled using custom MATLAB scripts developed by Dr. Daniel Stolzberg

612 (https://github.com/dstolz/epsych) and using a multifunction processor (RZ6; Tucker-Davis
613 Technologies).
614
615 *Procedural training*
616 Animals were trained on an amplitude modulation (AM) depth detection task using an aversive
617 conditioning Go/Nogo procedure used in the laboratory (Sarro and Sanes, 2010, 2011; Sarro et
618 al., 2011; Rosen et al., 2012; Buran et al., 2014a; Caras and Sanes, 2015, 2017). Gerbils were
619 placed on controlled water access and trained to drink from a waterspout in the presence of
620 continuous unmodulated noise (60 dB SPL; band-limited white noise, 3-20 kHz; Nogo/"Safe"
621 stimulus), and to refrain from drinking when the unmodulated noise transitioned to a 5 Hz AM rate
622 signal (Go/"Warn" stimulus). This was done by pairing the AM signal with a mildly aversive shock
623 (300 ms; 0.5-1.0 mA; Lafayette Instruments) delivered through the waterspout. Modulated, "warn"
624 trials (1 sec AM stimulus) were randomly interspersed with 3-5 unmodulated, "safe" trials (1 sec
625 trial duration) to deter temporal conditioning. First, animals were trained on the most salient AM
626 cue (100% modulated depth). Behavioral responses were classified as a "hit" if the animal
627 correctly withdrew from waterspout during modulated warn trials and as a "false alarm" if the
628 animal incorrectly withdrew from waterspout during unmodulated safe trials (see schematic in
629 Figure 2A). Behavioral performance was quantified using the signal detection metric, *d'*, defined
630 as $d' = z(\text{hit rate}) - z(\text{false alarm rate})$ (Green and Swets, 1966). Animals achieved task
631 proficiency when $d' \geq 1.5$ and completed three separate training sessions with a sufficient number
632 of warn trials (≥ 50). On the final session of procedural training, the sound level was lowered to
633 45 dB SPL.
634
635 *Perceptual testing*
636 Once animals reached the training performance criterion ($d' \geq 1.5$), animals were then
637 perceptually tested on a range of AM depths, from fully modulated (100% AM) to shallow
638 modulations (> 0% AM). Note, AM depths were presented on a dB scale (re: 100% depth), where
639 0 dB (re: 100% AM) refers to fully modulated noise (100%) and decreasing (negative) values refer
640 to smaller depths. These values are not to be confused with overall stimulus intensity, which
641 remained at 45 dB SPL during perceptual testing. Furthermore, the gain of the AM stimuli was
642 adjusted to accommodate for changes in average power across modulation depth (Wakefield and
643 Viemeister, 1990). Perceptual performance was assessed over ≥10 testing sessions. For each
644 session, the range of AM depths presented was adjusted to bracket the animal's detection
645 threshold, which was defined as the AM depth at which $d'=1$.

Psychometric analysis

Classified behavioral responses (i.e., Hits, False alarms) were used to generate psychometric functions used to determine AM depth detection thresholds. First, psychometric functions based on the percentage of Hits were plotted as a function of AM depth and fit with cumulative Gaussian using Bayesian inference (open-source MATLAB package psignifit 4) (Schütt et al., 2016; Caras and Sanes, 2017; Yao and Sanes, 2018). The default priors in psignifit 4 were used as it fit the behavioral data with high accuracy. Psychometric fits were then transformed to *d'* values (*d'* = *z(hit rate) – z(false alarm rate)*(Green and Swets, 1966). Psychometric functions using d' were used to determine AM depth detection thresholds, which was defined as the AM depth at which *d'=1*. When computing *d'*, we constrained the hit and false alarm rates (floor: 0.05; ceiling: 0.95) to avoid *d'* values that approached infinity (Caras and Sanes, 2017; Yao and Sanes, 2018).

In vivo neurophysiology

Electrode implantation

The procedural details for electrode implantation were identical to the procedures used in previous studies from our laboratory (Buran et al., 2014b; von Trapp et al., 2016; Caras and Sanes, 2017; Yao and Sanes, 2018). The procedures are briefly described below.

Following behavioral assessment, a subset of animals (Control: n=7; HL: n=9) were implanted with a multichannel electrode array in the primary auditory cortex (AC). Animals were anesthetized with isoflurane/O2 and secured on a stereotaxic apparatus (Kopf). The skull was exposed and a craniotomy was made on the dorsal skull at established coordinates for targeting the left core AC. The left cortex was targeted as it is more responsive to temporal acoustic features (Heffner and Heffner, 1984) A 64 channel silicone probe array (Neuronexus: Buzsaki64-5x12_H64LP_30mm
or A4x16-Poly2-5mm-23s-200-177-H64LP_30mm) was implanted into the AC and oriented such that the array spanned the tonotopic axis (Ter-Mikaelian et al., 2007; Rosen et al., 2012; von Trapp et al., 2016). The array was positioned at a 25º angle in the mediolateral plane, and the rostral-most probe shank was positioned at 3.9 mm rostral and 4.6-4.9 mm lateral to lambda. The array was fixed to a custom-made microdrive to allow for later advancement of the electrode across multiple behavioral testing days. Following recovery, neural recordings were made while animals performed the AM detection task. When all testing was complete, animals were deeply anesthetized, perfused with fixative (phosphate-buffered saline, 4% paraformaldehyde), brain

680 extracted, sectioned (Leica vibratome), and stained with Nissl dye. Electrode track position in the
681 core AC was verified using a gerbil brain atlas (Radtke-Schuller et al., 2016).
682
683 *Data acquisition*
684 Extracellular recordings were acquired using a wireless recording system (Triangle BioSystems)
685 while animals performed the AM detection task. Signals from all channels were pre-amplified,
686 digitized (24.4 kHz; PZ5; Tucker Davis Technologies, TDT), and sent to the RZ2 (TDT) for filtering
687 and processing. All recordings were pre-processed and sorted offline. First, recordings were pre-
688 processed using custom MATLAB scripts and initial spike thresholding was performed. Spikes
689 were semi-automatically sorted using Kilosort, a spike sorting framework based on template
690 matching of spike waveforms (Pachitariu et al., 2016). Spike waveforms were manually inspected
691 and refined in Phy (Rossant et al., 2016). Units were classified as single units if they were well-
692 isolated, displayed clear separation in PC space, and had few refractory period violations (<10%).
693 Units that did not meet criteria for single unit classification were classified as multi-units. Sorted
694 spike data were then analyzed using custom MATLAB scripts.
695
696 *Neurometric analysis*
697 Procedures for assessment of neural AM detection are similar to that described previously in the
698 laboratory (Caras and Sanes, 2017). Briefly, the firing rate (spikes / second) for each unit was
699 calculated over a 1 second duration for modulated and unmodulated stimuli. The 1 sec time period
700 corresponds to the duration of each trial. Neural *d'* values were computed based on the firing rate,
701 where for each AM depth, the firing rate was normalized by the standard deviation pooled across
702 all the stimuli (i.e., z-score), and subtracting the unmodulated value from each AM stimulus (d'_{FR}=
703 z(AM Depth) - z(Unmodulated)).
704
705 The neural *d'* values were used to generate neurometric functions, where the data were fit with a
706 logistic function using a nonlinear least-squares regression procedure (MATLAB function *nlinfit*).
707 See Supplementary Figure 2C for fit of neural d' data for two example neurometric functions. The
708 neurometric fit was deemed appropriate if the correlation between the predicted and actual d'
709 values were statistically significant (Pearson's *r*). As with the perceptual definition, AM detection
710 thresholds for each unit was defined as the AM depth at which *d'*=1. Units were classified as AM
711 responsive if (1) the neurometric fit was significant and (2) the maximum neural *d'* value is ≥1. All
712 other units that did not meet the criteria for AM responsivity were classified as unresponsive.
713

In addition, the strength of synchronization of unit responses to the envelope of each AM stimulus was quantified using a vector strength (VS) metric (Goldberg and Brown, 1969). Spikes occurring at the same phase of the AM resulted in high synchrony (VS=1) whereas spikes out of phase resulted in low synchrony (VS=0). The Rayleigh test of uniformity was used to determine statistical significance of the VS (Mardia, 1972) at the level of $p<0.001$.

Population coding

We used a previously employed linear classifier readout procedure (Yao and Sanes, 2018) to assess AM detection across a population of AC neurons. A linear classifier was trained to decode responses from a proportion of trials to each stimulus set (e.g., “Warn” and “Safe”; Figure 5A). Specifically, spike count responses from all neurons were counted across 1000 ms from "T" trials of "S" stimuli (e.g., AM depth) and formed the population "response vector". Since the number of trials were unequal across all units, we randomly subsampled a proportion of trials (i.e., 8 trials) from each unit. 7 of the 8 trials were then randomly sampled (without replacement) across all neurons. A support vector machine (SVM) procedure was used to fit a linear hyperplane to the data set ("training set"). Cross-validated classification performance was assessed on the remaining single trial (1 of the 8 trials) by computing the number of times this test set was correctly classified and misclassified based on the linear hyperplane across 500 iterations with a new randomly drawn sampled train and test sets for each iteration. Performance metrics were computed to determine the “Hit” rate (proportion of correctly classified Warn trials) and “False Alarm” rate (proportion of misclassified Safe trials). Similar to the psychometric and individual unit neurometric analyses, we converted population decoder performance metrics into d' values. The SVM procedure was implemented in MATLAB using the “fitcsvm” and “predict” functions with the “KernelFunction” set to “linear”.

Histology

After all electrophysiology experiments, animals were given an overdose of sodium pentobarbital (150 mg/kg, intraperitoneal injection) and perfused with 0.01 M phosphate-buffered saline followed by 4% paraformaldehyde. The brains were extracted, post-fixed in 4% paraformaldehyde, and embedded in 6% agar and sectioned at 60 µm on a vibratome (Lieca). Tissue sections were mounted on gelatin-subbed glass slides, dried, and stained for Nissl. Brightfield images were acquired using an upright microscope (Revolve, Echo) and electrode tracks were reconstructed offline and compared with a gerbil brain atlas (Radtke-Schuller et al., 2016) to confirm the electrodes targeted core auditory cortex (Figure 4B).

748

749 In vitro electrophysiology

750

751 *Thalamocortical brain slice preparation*

752 Following behavioral data collection, a subset of animals (Control: n=5; HL: n=5) were used for *in*
753 *vitro* auditory cortex (AC) recordings. The procedures for brain slice physiology experiments have
754 been established in prior studies from our laboratory (Kotak, 2005; Xu et al., 2007; Takesian et
755 al., 2012; Mowery et al., 2015). Animals were deeply anesthetized (400 mg/kg, chloral hydrate,
756 intraperitoneal) and brains extracted and placed into 4ºC oxygenated artificial cerebrospinal fluid
757 (ACSF, in mM: 125 NaCl, 4 KCl, 1.2 KH2PO4, 1.3 MgSO4, 26 NaHCO3, 15 glucose, 2.4 CaCl2,
758 and 0.4 L-ascorbic acid, pH=7.4 after bubbling with 95% O2/5% CO2). Brains were sectioned
759 horizontally (500 µm) to preserve the ventral medial geniculate (MGv) to AC projections.
760 Recording electrodes were fabricated from borosilicate glass microcapillaries with a micropipette
761 puller (Sutter). Before each whole-cell recording, the AC was identified by extracellular field
762 responses to MGv stimulation.

763

764 *Whole-cell current clamp recordings*

765 Current-clamp recordings were obtained (Warner, PC-501A) to assess inhibitory postsynaptic
766 potentials (IPSPs), excitatory postsynaptic potentials (EPSPs), and intrinsic firing rate in L2/3 AC
767 pyramidal neurons. IPSPs were evoked via local biphasic stimulation of layer 4 (1 ms, 1-10 mV)
768 in the presence of ionotropic glutamate receptor antagonists (20 µm DNQX; 50 µm AP-5).
769 Antagonists were applied at least 8 min prior to IPSP recordings. Peak IPSP amplitudes of the
770 short-latency hyperpolarization (putative $GABA_A$ component) and long-latency hyperpolarization
771 (putative $GABA_B$ component) were measured from each response at a holding potential (V_{hold})
772 of -50 mV. EPSPs were electrically evoked from L2/3 pyramidal cells at a holding potential (V_{hold})
773 of -80 mV. EPSP waveforms were collected with increasing afferent stimulation levels (0.1 – 1
774 mA). Maximum amplitudes were determined from EPSP waveforms for each stimulation level to
775 compute input-output functions. Action potential threshold was determined by delivering
776 incremental current pulses (1500 ms; 10 pA steps; 0.2 Hz) until a spike was evoked. Frequency-
777 current curves were collected by injecting depolarizing current steps (100-600 pA, 100 pA steps).
778 Recordings were digitized at 10 kHz and analyzed offline using custom Igor-based macros (IGOR,
779 WaveMetrics).

780

781

782 Auditory brainstem response (ABR) measurements

783 ABRs were collected from all control and adolescent HL animals to determine whether the long
784 duration of earplug insertion resulted in changes to the auditory periphery. ABR measurement
785 procedures were identical to those used in previous studies in our laboratory (Rosen et al., 2012;
786 Caras and Sanes, 2015; Yao and Sanes, 2018). ABRs were collected in animals following
787 behavioral data collection and prior to electrophysiological experiments (see timeline in Figure
788 1A). Animals were anesthetized with intraperitoneal injections of ketamine (30 mg/kg; Bioniche
789 Pharma) and pentobarbital (50 mg/kg; Sigma-Aldrich) and placed in a sound attenuation booth
790 (Industral Acoustics). Recordings were made with subdermal needle electrodes inserted at the
791 apex of the skull (positive electrode), the nape of the neck (inverting electrode; caudal to right
792 pinna), and ground in hind leg. Sound-evoked ABR signals were preamplified (10,000x) and band-
793 pass filtered (0.3-3 kHz) using a P55 model preamplifier (Grass Technologies). Signals were
794 additionally amplified (32 dB gain; Brownlee 440 amplifier) before digitizing at a 24.4 kHz sampling
795 rate (RZ6, TDT). Acoustic stimuli and data acquisition were controlled via custom Python scripts
796 running on a PC (scripts provided by Brandon Warren and Edwin Rubel, University of
797 Washington, Seattle). All stimuli were presented from a calibrated free-field speaker positioned
798 26 cm above the animal. Tone-evoked ABRs were collected by presenting tone pips (5 ms
799 duration; 2 ms linear rise-fall times) with frequencies that spanned the range of the gerbil
800 audiogram (0.5, 1, 2, 4, 6, 8, 16 kHz) (Ryan, 1976). Responses were averaged across 250-500
801 repetitions for each stimulus condition. Tone-ABR audiograms were generated by assessing the
802 ABR threshold at each test frequency. We defined the ABR threshold to be the lowest sound level
803 required to elicit a visually discernable ABR peak waveform. ABR waveforms exhibit stereotyped
804 peaks that are representative of summed peripheral auditory nuclei electrical activity. Here, we
805 focused on wave I of the ABR, which is thought to be generated by the auditory nerve (Jewett,
806 1970). We determined the peak of wave I amplitude, which is calculated as the absolute voltage
807 difference between the peak and the following trough. Wave I amplitude was computed as a
808 function of sound level to generate ABR input-output functions, which allowed us to assess
809 whether earplugs induced subtle damage to auditory nerve synapses (Liberman and Kujawa,
810 2017).
811
812 *Statistics*
813 Statistical analyses and procedures were performed using JMP Pro 15.0 (SAS) or custom-written
814 MATLAB scripts utilizing the Statistics and Curve Fitting Toolboxes. For normally distributed data
815 (assessed using Shapiro-Wilk Goodness of Fit Test), values are given as mean ± SEM. Non-

816 normally distributed data are given as median ± Quartile. Unless otherwise noted, all normally
817 distributed data were assessed using parametric procedures (i.e., ANOVA) followed by
818 appropriate *post hoc* controls for multiple comparisons (Tukey-Kramer HSD) when necessary.

References

Banai K, Sabin AT, Wright BA (2011) Separable developmental trajectories for the abilities to detect auditory amplitude and frequency modulation. Hear Res 280:219–227.

Barreira-Nielsen C, Fitzpatrick E, Hashem S, Whittingham JA, Barrowman N, Aglipay M (2016) Progressive hearing loss in early childhood. Ear Hear 37:e311–e321.

Bishop DVM, Hardiman M, Uwer R, Von Suchodoletz W (2007) Maturation of the long-latency auditory ERP: step function changes at start and end of adolescence. Dev Sci 10:565–575.

Bishop C V, Reiter TE, Erikson DW, Hanna CB, Daughtry BL, Chavez SL, Hennebold JD, Stouffer RL (2019) Chronically elevated androgen and/or consumption of a Western-style diet impairs oocyte quality and granulosa cell function in the nonhuman primate periovulatory follicle. J Assist Reprod Genet 36:1497–1511.

Blakemore S-J (2012) Development of the social brain in adolescence. J R Soc Med 105:111–116.

Brugge JF, Orman SS, Coleman JR, Chan JCK, Phillips DP (1985) Binaural interactions in cortical area AI of cats reared with unilateral atresia of the external ear canal. Hear Res 20:275–287.

Buran BN, Sarro EC, Manno FAM, Kang R, Caras ML, Sanes DH (2014a) A Sensitive Period for the Impact of Hearing Loss on Auditory Perception. J Neurosci 34:2276–2284.

Buran BN, von Trapp G, Sanes DH (2014b) Behaviorally Gated Reduction of Spontaneous Discharge Can Improve Detection Thresholds in Auditory Cortex. J Neurosci 34:4076 LP – 4081.

Burke AR, McCormick CM, Pellis SM, Lukkes JL (2017) Impact of adolescent social experiences on behavior and neural circuits implicated in mental illnesses. Neurosci Biobehav Rev 76:280–300.

Caras ML, Sanes DH (2015) Sustained Perceptual Deficits from Transient Sensory Deprivation. J Neurosci 35:10831–10842.

Caras ML, Sanes DH (2017) Top-down modulation of sensory cortex gates perceptual learning. Proc Natl Acad Sci 114:201712305.

Caras ML, Sanes DH (2019) Neural Variability Limits Adolescent Skill Learning. J Neurosci 39:2889 LP – 2902.

Carey S, Diamond R, Woods B (1980) Development of face recognition: A maturational component? Dev Psychol 16:257–269.

Cheetham CE, Belluscio L (2014) An Olfactory Critical Period. Science (80-) 344:157 LP – 158.

Christakis DA, Ramirez JSB, Ramirez JM (2012) Overstimulation of newborn mice leads to

853 behavioral differences and deficits in cognitive performance. Sci Rep 2:546.
854 Clements M, Kelly JB (1978) Auditory Spatial Responses of Young Guinea-Pigs (Cavia-
855 Porcellus) During and After Ear Blocking. J Comp Physiol Psychol 92:34–44.
856 Clopton BM, Silverman MS (1977) Plasticity of binaural interaction. II. Critical period and
857 changes in midline response. J Neurophysiol 40:1275–1280.
858 Cohen Kadosh K, Johnson MH, Dick F, Cohen Kadosh R, Blakemore S-J (2013) Effects of Age,
859 Task Performance, and Structural Brain Development on Face Processing. Cereb Cortex
860 23:1630–1642.
861 Danneman PJ, Suckow MA, Brayton C (2012) The laboratory mouse. CRC Press.
862 Davidson LL, Grigorenko EL, Boivin MJ, Rapa E, Stein A (2015) A focus on adolescence to
863 reduce neurological, mental health and substance-use disability. Nature 527:S161–S166.
864 Dayanidhi S, Hedberg Å, Valero-Cuevas FJ, Forssberg H (2013) Developmental improvements
865 in dynamic control of fingertip forces last throughout childhood and into adolescence. J
866 Neurophysiol 110:1583–1592.
867 de Villers-Sidani E, Chang EF, Bao S, Merzenich MM (2007) Critical Period Window for Spectral
868 Tuning Defined in the Primary Auditory Cortex (A1) in the Rat. J Neurosci 27:180 LP – 189.
869 Downes M, Bathelt J, De Haan M (2017) Event-related potential measures of executive
870 functioning from preschool to adolescence. Dev Med Child Neurol 59:581–590.
871 Eiland L, Romeo RD (2013) Stress and the developing adolescent brain. Neuroscience
872 249:162–171.
873 Einon DF, Morgan MJ (1977) A critical period for social isolation in the rat. Dev Psychobiol J Int
874 Soc Dev Psychobiol 10:123–132.
875 Fitzgerald MB, Wright BA (2011) Perceptual learning and generalization resulting from training
876 on an auditory amplitude-modulation detection task. J Acoust Soc Am 129:898–906.
877 Furman AC, Kujawa SG, Charles Liberman M (2013) Noise-induced cochlear neuropathy is
878 selective for fibers with low spontaneous rates. J Neurophysiol 110:577–586.
879 Gay JD, Voytenko S V, Galazyuk A V, Rosen MJ (2014) Developmental hearing loss impairs
880 signal detection in noise: putative central mechanisms. Front Syst Neurosci 8:162.
881 Germine LT, Duchaine B, Nakayama K (2011) Where cognitive development and aging meet:
882 Face learning ability peaks after age 30. Cognition 118:201–210.
883 Giedd JN, Blumenthal J, Jeffries NO, Castellanos FX, Liu H, Zijdenbos A, Paus T, Evans AC,
884 Rapoport JL (1999) Brain development during childhood and adolescence: a longitudinal
885 MRI study. Nat Neurosci 2:861–863.
886 Goldberg JM, Brown PB (1969) Response of binaural neurons of dog superior olivary complex

887 to dichotic tonal stimuli: some physiological mechanisms of sound localization. J
888 Neurophysiol 32:613–636.
889 Green DB, Mattingly MM, Ye Y, Gay JD, Rosen MJ (2017) Brief Stimulus Exposure Fully
890 Remediates Temporal Processing Deficits Induced by Early Hearing Loss. J Neurosci
891 37:7759 LP – 7771.
892 Green DM, Swets JA (1966) Signal detection theory and psychophysics. New York-London-
893 Sydney: John Wiley & Sons.
894 Guyer AE, Monk CS, McClure-Tone EB, Nelson EE, Roberson-Nay R, Adler AD, Fromm SJ,
895 Leibenluft E, Pine DS, Ernst M (2008) A Developmental Examination of Amygdala
896 Response to Facial Expressions. J Cogn Neurosci 20:1565–1582.
897 Hall JW, Grose JH, Pillsbury HC (1995) Long-term effects of chronic otitis media on binaural
898 hearing in children. Arch Otolaryngol Neck Surg 121:847–852.
899 Han YK, Köver H, Insanally MN, Semerdjian JH, Bao S (2007) Early experience impairs
900 perceptual discrimination. Nat Neurosci 10:1191–1197.
901 Heffner HE, Heffner RS (1984) Temporal lobe lesions and perception of species-specific
902 vocalizations by macaques. Science (80-) 226:75–76.
903 Hensch TK (2005) Critical period plasticity in local cortical circuits. Nat Rev Neurosci 6:877–888.
904 Hubel DH, Wiesel TN (1970) The period of susceptibility to the physiological effects of unilateral
905 eye closure in kittens. J Physiol 206:419–436.
906 Huyck JJ, Wright BA (2011) Late maturation of auditory perceptual learning. Dev Sci 14:614–
907 621.
908 Huyck JJ, Wright BA (2013) Learning, worsening, and generalization in response to auditory
909 perceptual training during adolescence. J Acoust Soc Am 134:1172–1182.
910 Ihlefeld A, Chen Y-W, Sanes DH (2016) Developmental Conductive Hearing Loss Reduces
911 Modulation Masking Release. Trends Hear 20:1–14.
912 Isgor C, Kabbaj M, Akil H, Watson SJ (2004) Delayed effects of chronic variable stress during
913 peripubertal-juvenile period on hippocampal morphology and on cognitive and stress axis
914 functions in rats. Hippocampus 14:636–648.
915 Jain S, Ashworth J, Biswas S, Lloyd IC (2010) Duration of form deprivation and visual outcome
916 in infants with bilateral congenital cataracts. J AAPOS 14:31–34.
917 Jewett DL (1970) Volume-conducted potentials in response to auditory stimuli as detected by
918 averaging in the cat. Electroencephalogr Clin Neurophysiol 28:609–618.
919 Kadosh KC, Linden DEJ, Lau JYF (2013) Plasticity during childhood and adolescence:
920 innovative approaches to investigating neurocognitive development. Dev Sci 16:574–583.

921 Keating P, Dahmen JC, King AJ (2013) Context-Specific Reweighting of Auditory Spatial Cues
922 following Altered Experience during Development. Curr Biol 23:1291–1299.
923 Keating P, Dahmen JC, King AJ (2015a) Complementary adaptive processes contribute to the
924 developmental plasticity of spatial hearing. Nat Neurosci 18:185–187.
925 Keating P, Dahmen JC, King AJ (2015b) Complementary adaptive processes contribute to the
926 developmental plasticity of spatial hearing. Nat Neurosci 18:185.
927 Kim JH, Li S, Richardson R (2011) Immunohistochemical Analyses of Long-Term Extinction of
928 Conditioned Fear in Adolescent Rats. Cereb Cortex 21:530–538.
929 Knudsen EI (1983) Early auditory experience aligns the auditory map of space in the optic
930 tectum of the barn owl. Science (80-) 222:939 LP – 942.
931 Knudsen EI (1985) Experience alters the spatial tuning of auditory units in the optic tectum
932 during a sensitive period in the barn owl. J Neurosci 5:3094–3109.
933 Knudsen EI, Esterly SD, Knudsen PF (1984a) Monaural occlusion alters sound localization
934 during a sensitive period in the barn owl. J Neurosci 4:1001–1011.
935 Knudsen EI, Knudsen PF, Esterly SD (1982) Early auditory experience modifies sound
936 localization in barn owls. Nature 295:238–240.
937 Knudsen EI, Knudsen PF, Esterly SD (1984b) A critical period for the recovery of sound
938 localization accuracy following monaural occlusion in the barn owl. J Neurosci 4:1012–
939 1020.
940 Kotak VC (2005) Hearing Loss Raises Excitability in the Auditory Cortex. J Neurosci 25:3908–
941 3918.
942 Lebel C, Beaulieu C (2011) Longitudinal Development of Human Brain Wiring Continues from
943 Childhood into Adulthood. J Neurosci 31:10937 LP – 10947.
944 Lewis TL, Maurer D (2005) Multiple sensitive periods in human visual development: Evidence
945 from visually deprived children. Dev Psychobiol 46:163–183.
946 Liberman MC, Kujawa SG (2017) Cochlear synaptopathy in acquired sensorineural hearing
947 loss: Manifestations and mechanisms. Hear Res 349:138–147.
948 Lü J, Huang Z, Yang T, Li Y, Mei L, Xiang M, Chai Y, Li X, Li L, Yao G, Wang Y, Shen X, Wu H
949 (2011) Screening for delayed-onset hearing loss in preschool children who previously
950 passed the newborn hearing screening. Int J Pediatr Otorhinolaryngol 75:1045–1049.
951 Mahajan Y, McArthur G (2012a) Maturation of visual evoked potentials across adolescence.
952 Brain Dev 34:655–666.
953 Mahajan Y, McArthur G (2012b) Maturation of auditory event-related potentials across
954 adolescence. Hear Res 294:82–94.

955 Mann VA, Diamond R, Carey S (1979) Development of voice recognition: Parallels with face
956 recognition. J Exp Child Psychol 27:153–165.
957 Mardia K V (1972) Statistics of directional data Academic Press. New York 357.
958 McCallum J, Kim JH, Richardson R (2010) Impaired Extinction Retention in Adolescent Rats:
959 Effects of D-Cycloserine. Neuropsychopharmacology 35:2134–2142.
960 McKenna Benoit M, Orlando M, Henry K, Allen P (2018) Amplitude Modulation Detection in
961 Children with a History of Temporary Conductive Hearing Loss Remains Impaired for
962 Years After Restoration of Normal Hearing. J Assoc Res Otolaryngol 20:89–98.
963 McMurray B, Danelz A, Rigler H, Seedorff M (2018) Speech categorization develops slowly
964 through adolescence. Dev Psychol 54:1472–1491.
965 Mogdans J, Knudsen EI (1992) Adaptive adjustment of unit tuning to sound localization cues in
966 response to monaural occlusion in developing owl optic tectum. J Neurosci 12:3473 LP –
967 3484.
968 Mogdans J, Knudsen EI (1993) Early monaural occlusion alters the neural map of interaural
969 level differences in the inferior colliculus of the barn owl. Brain Res 619:29–38.
970 Moore DR, Hine JE, Jiang ZD, Matsuda H, Parsons CH, King AJ (1999) Conductive Hearing
971 Loss Produces a Reversible Binaural Hearing Impairment. 19:8704–8711.
972 Moore DR, Irvine DRF (1981) Plasticity of binaural interaction in the cat inferior colliculus. Brain
973 Res 208:198–202.
974 Moore JK, Guan YL (2001) Cytoarchitectural and axonal maturation in human auditory cortex.
975 JARO - J Assoc Res Otolaryngol 2:297–311.
976 Mowery TM, Caras ML, Hassan SI, Wang DJ, Dimidschstein J, Fishell G, Sanes DH (2019)
977 Preserving Inhibition during Developmental Hearing Loss Rescues Auditory Learning and
978 Perception. J Neurosci 39:8347 LP – 8361.
979 Mowery TM, Kotak VC, Sanes DH (2015) Transient Hearing Loss Within a Critical Period
980 Causes Persistent Changes to Cellular Properties in Adult Auditory Cortex. Cereb Cortex
981 25:2083–2094.
982 Mowery TM, Penikis KB, Young SK, Ferrer CE, Kotak VC, Sanes DH (2017) The Sensory
983 Striatum Is Permanently Impaired by Transient Developmental Deprivation. Cell Rep
984 19:2462–2468.
985 Niskar AS, Kieszak SM, Holmes AE, Esteban E, Rubin C, Brody DJ (2001) Estimated
986 Prevalence of Noise-Induced Hearing Threshold Shifts Among Children 6 to 19 Years of
987 Age: The Third National Health and Nutrition Examination Survey, 1988–1994, United
988 States. Pediatrics 108:40 LP – 43.

Norris M, Adams C (1974) Sexual development in the Mongolian gerbil, Meriones unguiculatus, with particular reference to the ovary. Reproduction 36:245–248.

Pachitariu M, Steinmetz N, Kadir S, Carandini M, Harris K (2016) Fast and accurate spike sorting of high-channel count probes with KiloSort. Adv Neural Inf Process Syst:4455–4463.

Patel SR, Bouldin E, Tey CS, Govil N, Alfonso KP (2020) Social Isolation and Loneliness in the Hearing-Impaired Pediatric Population: A Scoping Review. Laryngoscope.

Pattwell SS, Duhoux S, Hartley CA, Johnson DC, Jing D, Elliott MD, Ruberry EJ, Powers A, Mehta N, Yang RR (2012) Altered fear learning across development in both mouse and human. Proc Natl Acad Sci 109:16318–16323.

Paus T, Keshavan M, Giedd JN (2008) Why do many psychiatric disorders emerge during adolescence? Nat Rev Neurosci 9:947–957.

Petanjek Z, Judaš M, Šimić G, Rašin MR, Uylings HBM, Rakic P, Kostović I (2011) Extraordinary neoteny of synaptic spines in the human prefrontal cortex. Proc Natl Acad Sci 108:13281 LP – 13286.

Pinto-Fochi ME, Negrin AC, Scarano WR, Taboga SR, Góes RM (2016) Sexual maturation of the Mongolian gerbil (*Meriones unguiculatus*): a histological, hormonal and spermatic evaluation. Reprod Fertil Dev 28:815–823.

Pinto (2010) Developmental changes in GABAergic mechanisms in human visual cortex across the lifespan. Front Cell Neurosci 4:1–12.

Pitkow X, Liu S, Angelaki DE, DeAngelis GC, Pouget A (2015) How Can Single Sensory Neurons Predict Behavior? Neuron 87:411–423.

Polley DB, Thompson JH, Guo W (2013) Brief hearing loss disrupts binaural integration during two early critical periods of auditory cortex development. Nat Commun 4:2547.

Popescu M V., Polley DB (2010) Monaural Deprivation Disrupts Development of Binaural Selectivity in Auditory Midbrain and Cortex. Neuron 65:718–731.

Putzar L, Hötting K, Röder B (2010) Early visual deprivation affects the development of face recognition and of audio-visual speech perception. Restor Neurol Neurosci 28:251–257.

Putzar L, Hötting K, Rösler F, Röder B (2007) The development of visual feature binding processes after visual deprivation in early infancy. Vision Res 47:2616–2626.

Radtke-Schuller S, Schuller G, Angenstein F, Grosser OS, Goldschmidt J, Budinger E (2016) Brain atlas of the Mongolian gerbil (Meriones unguiculatus) in CT/MRI-aided stereotaxic coordinates. Brain Struct Funct 221.

Rosen MJ, Sarro EC, Kelly JB, Sanes DH (2012) Diminished behavioral and neural sensitivity to

1023 sound modulation is associated with moderate developmental hearing loss. PLoS One 7.
1024 Rossant C, Kadir SN, Goodman DFM, Schulman J, Hunter MLD, Saleem AB, Grosmark A,
1025 Belluscio M, Denfield GH, Ecker AS, Tolias AS, Solomon S, Buzsáki G, Carandini M,
1026 Harris KD (2016) Spike sorting for large, dense electrode arrays. Nat Neurosci 19:634–
1027 641.
1028 Ryan A (1976) Hearing sensitivity of the mongolian gerbil, Meriones unguiculatis. J Acoust Soc
1029 Am 59:1222–1226.
1030 Sarro EC, Rosen MJ, Sanes DH (2011) Taking advantage of behavioral changes during
1031 development and training to assess sensory coding mechanisms. Ann N Y Acad Sci
1032 1225:142–154.
1033 Sarro EC, Sanes DH (2010) Prolonged maturation of auditory perception and learning in gerbils.
1034 Dev Neurobiol 70:636–648.
1035 Sarro EC, Sanes DH (2011) The Cost and Benefit of Juvenile Training on Adult Perceptual Skill.
1036 J Neurosci 31:5383 LP – 5391.
1037 Sawyer SM, Azzopardi PS, Wickremarathne D, Patton GC (2018) The age of adolescence.
1038 Lancet Child Adolesc Heal 2:223–228.
1039 Schütt HH, Harmeling S, Macke JH, Wichmann FA (2016) Painfree and accurate Bayesian
1040 estimation of psychometric functions for (potentially) overdispersed data. Vision Res
1041 122:105–123.
1042 Selemon LD (2013) A role for synaptic plasticity in the adolescent development of executive
1043 function. Transl Psychiatry 3:e238–e238 Available at: https://doi.org/10.1038/tp.2013.7.
1044 Shafer VL, Yu YH, Wagner M (2015) Maturation of cortical auditory evoked potentials (CAEPs)
1045 to speech recorded from frontocentral and temporal sites: Three months to eight years of
1046 age. Int J Psychophysiol 95:77–93.
1047 Shargorodsky J, Curhan SG, Curhan GC, Eavey R (2010) Change in prevalence of hearing loss
1048 in US adolescents. JAMA - J Am Med Assoc 304:772–778.
1049 Sharma A, Dorman MF, Spahr AJ (2002) A Sensitive Period for the Development of the Central
1050 Auditory System in Children with Cochlear Implants: Implications for Age of Implantation.
1051 Ear Hear 23.
1052 Sharma A, Kraus N, J. McGee T, Nicol TG (1997) Developmental changes in P1 and N1 central
1053 auditory responses elicited by consonant-vowel syllables. Electroencephalogr Clin
1054 Neurophysiol Potentials Sect 104:540–545.
1055 Silverman MS, Clopton BM (1977) Plasticity of binaural interaction. I. Effect of early auditory
1056 deprivation. J Neurophysiol 40:1266–1274.

1057 Simmonds DJ, Hallquist MN, Luna B (2017) Protracted development of executive and
1058 mnemonic brain systems underlying working memory in adolescence: A longitudinal fMRI
1059 study. Neuroimage 157:695–704.
1060 Singh NC, Theunissen FE (2003) Modulation spectra of natural sounds and ethological theories
1061 of auditory processing. J Acoust Soc Am 114:3394–3411.
1062 Smith RJH, Bale JF, White KR (2005) Sensorineural hearing loss in children. Lancet 365:879–
1063 890.
1064 Sussman E, Steinschneider M, Gumenyuk V, Grushko J, Lawson K (2008) The maturation of
1065 human evoked brain potentials to sounds presented at different stimulus rates. Hear Res
1066 236:61–79.
1067 Svirsky MA, Teoh S-W, Neuburger H (2004) Development of Language and Speech Perception
1068 in Congenitally, Profoundly Deaf Children as a Function of Age at Cochlear Implantation.
1069 Audiol Neurotol 9:224–233.
1070 Takesian AE, Kotak VC, Sanes DH (2012) Age-dependent effect of hearing loss on cortical
1071 inhibitory synapse function. J Neurophysiol 107:937–947.
1072 Ter-Mikaelian M, Sanes DH, Semple MN (2007) Transformation of Temporal Properties
1073 between Auditory Midbrain and Cortex in the Awake Mongolian Gerbil. J Neurosci
1074 27:6091–6102.
1075 Theunissen SCPM, Rieffe C, Netten AP, Briaire JJ, Soede W, Schoones JW, Frijns JHM (2014)
1076 Psychopathology and Its Risk and Protective Factors in Hearing-Impaired Children and
1077 Adolescents: A Systematic Review. JAMA Pediatr 168:170–177.
1078 Tomblin JB, Harrison M, Ambrose SE, Walker EA, Oleson JJ, Moeller MP (2015) Language
1079 outcomes in young children with mild to severe hearing loss. Ear Hear 36:76S-91S.
1080 Van der Loos H, Woolsey TA (1973) Somatosensory Cortex: Structural Alterations following
1081 Early Injury to Sense Organs. Science (80-) 179:395 LP – 398.
1082 Viemeister NF (1979) Temporal modulation transfer functions based upon modulation
1083 thresholds. J Acoust Soc Am 66:1364–1380.
1084 von Trapp G, Aloni I, Young S, Semple MN, Sanes DH (2017) Developmental hearing loss
1085 impedes auditory task learning and performance in gerbils. Hear Res 347:3–10.
1086 von Trapp G, Buran BN, Sen K, Semple MN, Sanes DH (2016) A Decline in Response
1087 Variability Improves Neural Signal Detection during Auditory Task Performance. J Neurosci
1088 36:11097–11106.
1089 Wakefield GH, Viemeister NF (1990) Discrimination of modulation depth of sinusoidal amplitude
1090 modulation (SAM) noise. J Acoust Soc Am 88:1367–1373.

1091 Xu H, Kotak VC, Sanes DH (2007) Conductive Hearing Loss Disrupts Synaptic and Spike
1092 Adaptation in Developing Auditory Cortex. J Neurosci 27:9417–9426.
1093 Xu L, Jen PH-S (2001) The effect of monaural middle ear destruction on postnatal development
1094 of auditory response properties of mouse inferior collicular neurons. Hear Res 159:1–13.
1095 Yao JD, Sanes DH (2018) Developmental deprivation-induced perceptual and cortical
1096 processing deficits in awake-behaving animals. Elife 7.
1097 Ye Y, Ihlefeld A, Rosen MJ (2021) Conductive hearing loss during development does not
1098 appreciably alter the sharpness of cochlear tuning. Sci Rep 11:3955.
1099 Yoshinaga-Itano C, Sedey AL, Coulter DK, Mehl AL (1998) Language of early- and later-
1100 identified children with hearing loss. Pediatrics 102:1161–1171.
1101 Zadeh LM, Silbert NH, Sternasty K, Swanepoel DW, Hunter LL, Moore DR (2019) Extended
1102 high-frequency hearing enhances speech perception in noise. Proc Natl Acad Sci
1103 116:23753–23759.
1104 Zhou X, Merzenich MM (2009) Developmentally degraded cortical temporal processing restored
1105 by training. Nat Neurosci 12:26–28.
1106 Zhuang X, Sun W, Xu-Friedman MA (2017) Changes in Properties of Auditory Nerve Synapses
1107 following Conductive Hearing Loss. J Neurosci 37.
1108
1109

Supplemental Figures

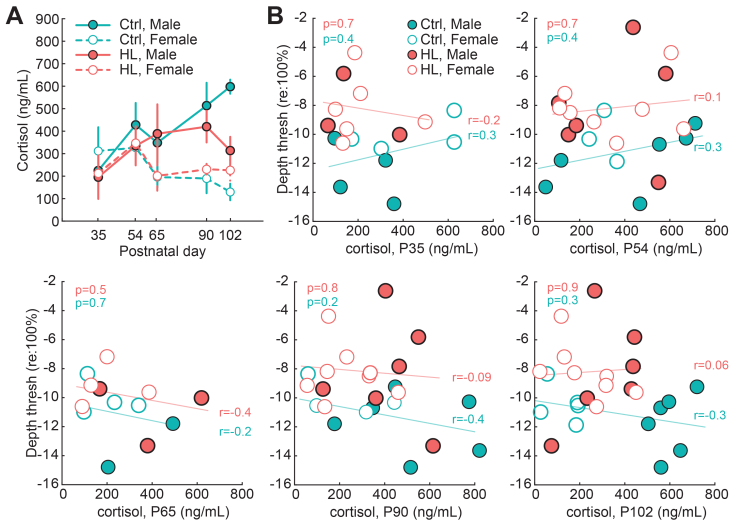

Supplementary Figure 1. Poorer behavioral detection thresholds are not due to elevated stress during adolescence. (**A**) Serum cortisol levels across age for male (solid line) and female (dotted line) gerbils. (**B**) Behavioral depth thresholds for the first day of perceptual testing (~P126; dB re: 100%) as a function of cortisol levels collected at P35, P54, P65, P90, and P102. Solid line indicates the linear fit for each group (Control, adolescent HL), along with the associated Pearson's *r* correlation value. The p-values of each linear fit are listed in the top left corner of each plot. Elevated cortisol levels at any of the ages collected do not correlate with poorer detection thresholds at P126.

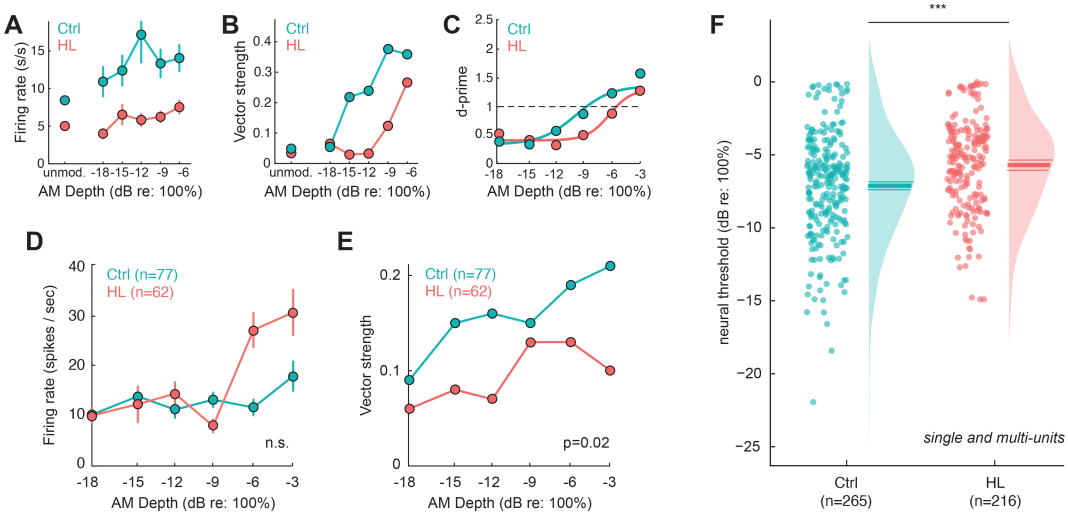

Supplementary Figure 2. Basic response properties and detection thresholds for individual auditory cortex neurons. (**A-C**) Firing rate (s/s), vector strength (VS), and d' values for example single units shown in Figure 4C. (**D-E**) Firing rate (s/s) and vector strength for a population of single units that met the criteria for AM sensitivity (same neurons from Figure 4). (**F**) Neural thresholds for single and multi units are plotted for control and HL animals. Individual thresholds are shown (circles), along with a half-violin plot indicating the probability density function. Horizontal lines indicate the mean±SEM. Individual single and multi units from HL animals exhibit poorer neural depth thresholds than control single units ($p<0.001$).

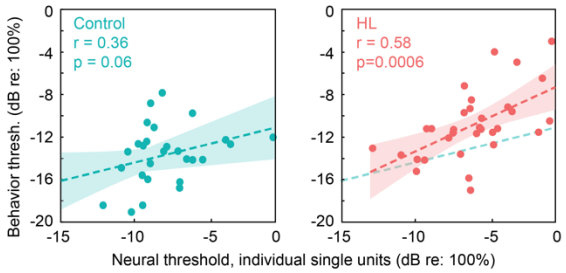

Supplementary Figure 3. Neural sensitivity of individual cortical neurons correlate with perceptual performance. Behavioral threshold as a function of neural thresholds for individual single units that meet the criteria for AM sensitivity (see Methods). The neural thresholds are the average threshold for single units per session (i.e., 1 avg / session). Dotted lines indicate a fitted linear regression, with shaded areas indicating the (± 1 SD) of the prediction error. Pearson's *r* and statistical significance of each fit are noted in the top left corner of each plot.

1111